Article

Proteolytic activation of fatty acid synthase signals pan-stress resolution

Check for updates

Hai Wei [1], Yi M. Weaver [1], Chendong Yang[2], Yuan Zhang [1], Guoli Hu[3], Courtney M. Karner [3], Matthew Sieber [4], Ralph J. DeBerardinis [2,5] & Benjamin P. Weaver [1]

Chronic stress and inflammation are both outcomes and major drivers of many human diseases. Sustained responsiveness despite mitigation suggests a failure to sense resolution of the stressor. Here we show that a proteolytic cleavage event of fatty acid synthase (FASN) activates a global cue for stress resolution in *Caenorhabditis elegans*. FASN is well established for biosynthesis of the fatty acid palmitate. Our results demonstrate FASN promoting an anti-inflammatory profile apart from palmitate synthesis. Redox-dependent proteolysis of limited amounts of FASN by caspase activates a C-terminal fragment sufficient to downregulate multiple aspects of stress responsiveness, including gene expression, metabolic programs and lipid droplets. The FASN C-terminal fragment signals stress resolution in a cell non-autonomous manner. Consistent with these findings, FASN processing is also seen in well-fed but not fasted male mouse liver. As downregulation of stress responses is critical to health, our findings provide a potential pathway to control diverse aspects of stress responses.

Alterations in nutrient availability, oxidative imbalances and exposures to cytotoxic substances or pollutants are all examples of cellular stressors. When faced with these insults, cells mount the relevant stress mitigation program to restore homeostasis. Outcomes include upregulating buffering factors such as chaperones, repairing damaged DNA, autophagy of cellular components or death of irreversibly damaged cells. Whether animals have a globally acting mechanism to detect the resolution of diverse stressors and signal the downregulation of multiple features of stress responses is unknown; however, such a mechanism would offer a survival advantage to limit loss of energy stores, speed wound healing and prepare the animal for encounters with another stressor. For multicellular organisms, coordinating stress recovery across tissues imposes additional challenges.

Adaptations to stressors not only require altered gene expression but also metabolic rewiring to repurpose energy stores. Metabolic adaptations to stressors can result in the generation of reactive oxygen species (ROS) or reactive nitrogen species. These reactive species cause extensive cellular damage including lipid peroxidation resulting in toxic aldehyde intermediates that further damage other macromolecules and lead to the death of tissues. Thus, lipids have an intriguing duality in stress responses as both energy stores and liability to damaging agents resulting in lipotoxicity. This underscores the need to have dynamic control of lipid availability but also safeguard the cell.

Cytosolic FASN is the biosynthetic enzyme responsible for the de novo synthesis of saturated fatty acids, the building blocks of fats and higher-order lipids[1,2]. Fat synthesis by FASN is a major pathway consuming energy stores in the form of NADPH. Notably, upregulation of *FASN* expression is a hallmark of tumorigenesis where tumor cells are thought to acquire de novo lipid synthesis[3]; however, it is not clear whether *FASN* upregulation solely reflects increased nutrient demand for growth as lipids are involved in multiple aspects of cellular transformation, including immune suppression and drug resistance, thereby preventing death of transformed cells[3].

Caspases are well known for activating proinflammatory cytokines or committing cells to programmed cell death if a genotoxic insult is not repaired. This same family of cysteine proteases also has

[1]Department of Pharmacology, UT Southwestern, Dallas, TX, USA. [2]Children's Medical Center Research Institute, UT Southwestern, Dallas, TX, USA. [3]Department of Internal Medicine, UT Southwestern, Dallas, TX, USA. [4]Department of Physiology, UT Southwestern, Dallas, TX, USA. [5]Howard Hughes Medical Institute, UT Southwestern, Dallas, TX, USA. ✉e-mail: benjamin.weaver@utsouthwestern.edu

ancient nonlethal roles in promoting differentiation; however, across metazoans, these same proteases have poorly understood roles in supporting homeostasis, where modulating caspase function alters stress resistance in *C. elegans*[4,5], reprograms cardiac hypertrophic responses in rats[6] and accelerates aging in mice[7]. Our previous work identified CED-3 caspase blocking a p38 MAPK-dependent epidermal pathogen response[5]. Also, the dual-leucine zipper kinase (DLK-1 and MAPK3K12) pathway was implicated downstream of caspase in neuronal regeneration following injury[8]. We and others recently showed that the relative extent of caspase activity can be neuroprotective by supporting organelle dynamics where caspase can limit TDP43 mitochondrial injury[9] or modulate p38 MAPK signaling to support lysosome formation[10]. Additionally, stress-induced caspase-2 cleavage of site 1 protease (S1P) triggers persistent activation of the transcription factor SREBP leading to NASH development[11]; however, for each of these cases, the caspase was found targeting a factor activating a stress response.

Beyond detecting an insult to activate a stress response, little is known how animals sense the resolution of stressors. Here we identify a signaling function of FASN that is independent of palmitate biosynthesis. We show that redox-dependent caspase cleavage of FASN serves as a sensing mechanism to gauge appropriate responses to diverse stressors. With cysteine active sites, the proteolytic activity of caspases can be inhibited by stressors in a redox-dependent manner. When the stressor is mitigated, limited amounts of the C-terminal fragment (CTF) act as a strong cue to downregulate widespread features of animal stress responses, analogous to an anti-inflammatory signal. Moreover, FASN-CTF enzymatic activity is required to suppress stress-responsive gene expression programs and promote lipid mobilization. Forced expression of FASN-CTF before stress amelioration compromises survival underscoring its function as a stress-resolution cue.

Results

Caspase controls diverse stress responses

Disrupting the caspase pathway in *C. elegans* provided us with a model to examine chronic stress responses. As early as 4 h of tunicamycin treatment, the *ced-3(-)* caspase and upstream activating Apaf gene *ced-4(-)* null mutants had dramatically enhanced induction of the Hsp70 family (HSPA5, BiP) endoplasmic reticulum (ER) stress marker HSP-4p::GFP relative to wild-type animals (Fig. 1a,b and Extended Data Fig. 1a,b). This enhanced response persisted to 2 d (Fig. 1b). Moreover, although the *ced-3(-)* and *ced-4(-)* null mutants normally develop slower than wild-type animals, both mutants had faster development under ER stress conditions compared to wild-type animals (Fig. 1c and Extended Data Fig. 1c), suggesting that the higher induction of HSP-4p::GFP reflects an enhanced survival advantage upon tunicamycin-induced ER stress.

We next sought to test whether *ced-3* and *ced-4* mutants would have similar persistent phenotypes with other stressors. Analogous to the heightened ER stress response, the *ced-3(-)* and *ced-4(-)* null mutants had dramatically enhanced induction of markers for both osmotic stress (NLP-29p::GFP) and ROS stress (GCS-1p::GFP) relative to wild-type animals when challenged with high salt and paraquat, respectively (Extended Data Figs. 1d–g and 2a–d).

The *ced-3(-)* and *ced-4(-)* mutants also had enhanced motility when given the salt challenge (Extended Data Fig. 2e,f) and enhanced survival on paraquat relative to wild-type animals (Extended Data Fig. 2g,h). Our findings are consistent with previous work showing that *ced-3* and *ced-4* mutants have enhanced survival with ER and osmotic stresses[4]. Notably, for each of the diverse stress challenges, wild-type animals never reached the same pronounced induction as seen with the *ced-3* caspase and *ced-4* Apaf mutants. Also, the *ced-3* and *ced-4* mutants had marked variability for the induction of the stress reporters. Together, these results indicate that caspase pathway normally regulates the overall magnitude of responsiveness to diverse stressors. We were

therefore intrigued to identify what target pathway is responsible for the enhanced pan-stress responsiveness.

FASN acts like caspase to limit stress responses

To reveal the caspase signaling target, we performed an RNA interference (RNAi) screen using the HSP-4p::GFP reporter with tunicamycin-induced ER stress to identify candidate factors contributing to persistently-heightened stress responses (Fig. 1d). The targeted screen examined established stress-responsive regulators and genes upregulated in stress (Extended Data Fig. 3a–c). The *C. elegans* FASN ortholog *fasn-1* gene acted like *ced-3(-)* and *ced-4(-)* mutants with enhanced induction and pronounced variability of HSP-4p::GFP expression under ER stress (Fig. 1e,f and Extended Data Fig. 3c). Moreover, because *fasn-1* RNAi knockdown did not enhance stress response in *ced-3(-)* mutants (Fig. 1f), we wanted to confirm that loss of FASN-1 expression acts like *ced-3(-)* null.

To confirm that the loss of FASN-1 function resulted in enhanced stress response in animals with intact CED-3 function, we used an alternative technique to deplete FASN at the protein level. We added hemagglutinin (HA)-labelled auxin-induced degron (AID) tags to both the N and C termini of the *fasn-1*-coding sequence in the endogenous genomic locus using CRISPR mutagenesis. When treated with auxin, the amount of FASN protein was significantly reduced (Extended Data Fig. 3d) and depletion enhanced induction of HSP-4p::GFP with ER stress (Fig. 1g), NLP-29p::GFP for osmotic stress (Fig. 1h) and GCS-1p::GFP for ROS stress (Fig. 1i). These effects were not due to TIR-1 E3 ligase expression, AID-tagging of FASN-1 or auxin treatment as these alone did not enhance the reporters (Extended Data Fig. 3e–g). Because the loss of *fasn-1* acted like the loss of *ced-3* caspase, we considered the possibility that FASN-1 could be acting downstream of CED-3 in limiting stress responses.

FASN proteolysis by caspase limits stress response

To confirm that the proteolytic activity of caspase is required for limiting stress responses, we used a proteolytic dead caspase active-site mutation G360S. This mutant generates a full-length CED-3 protein but lacks proteolytic activity. Consistent with *ced-3* null mutants, animals with proteolytic dead CED-3 also had enhanced stress reporter induction as well as survival under ER, osmotic and ROS stressors (Fig. 2a and Extended Data Fig. 4a–g). This finding suggests that the proteolytic activity of CED-3 is required for regulating stress response. It also explains the role of CED-4 Apaf in stress response as it promotes CED-3 proteolytic activity.

To test directly the cleavage of FASN-1 by CED-3, we divided *C. elegans* FASN-1 into three large peptide fragments and tested each with in vitro cleavage analyses (Fig. 2b). We identified a single CED-3 cleavage site for *C. elegans* FASN-1 in fragment 2 at Asp1593 toward the end of the long non-enzymatic linker region separating the N- and C-terminal enzymatic domains (Fig. 2c,d). Like all animal FASN proteins, the human FASN protein has the same domain architecture as *C. elegans* FASN-1 with long intervening non-enzymatic linker. Therefore, we similarly divided *Homo sapiens* FASN into three large peptide fragments. We found that human caspase-3 cleaved human FASN fragments 1 and 2 in vitro (Fig. 2e). This cleavage leaves an intact CTF, including most of the enoyl reductase (ER) domain and ketoacyl reductase (KR), acyl carrier protein (ACP) and thioesterase (TE) domains analogous to the cleavage location for *C. elegans* FASN-1. Furthermore, human caspase-3 and *C. elegans* CED-3 caspase are known to have similar proteolytic activities. Altogether these results indicate that the cleavage of FASN by caspase may be broadly conserved in metazoans.

To test whether the cleavage of FASN-1 by CED-3 is responsible for the enhanced stress responsiveness in vivo, we generated a FASN-1 cleavage-resistant mutation D1593E *'fasn-1(D/E)'* in the endogenous locus of *C. elegans fasn-1* using CRISPR mutagenesis. Using western blot, we first tested FASN-1 expression in wild-type, *ced-3(-)* and
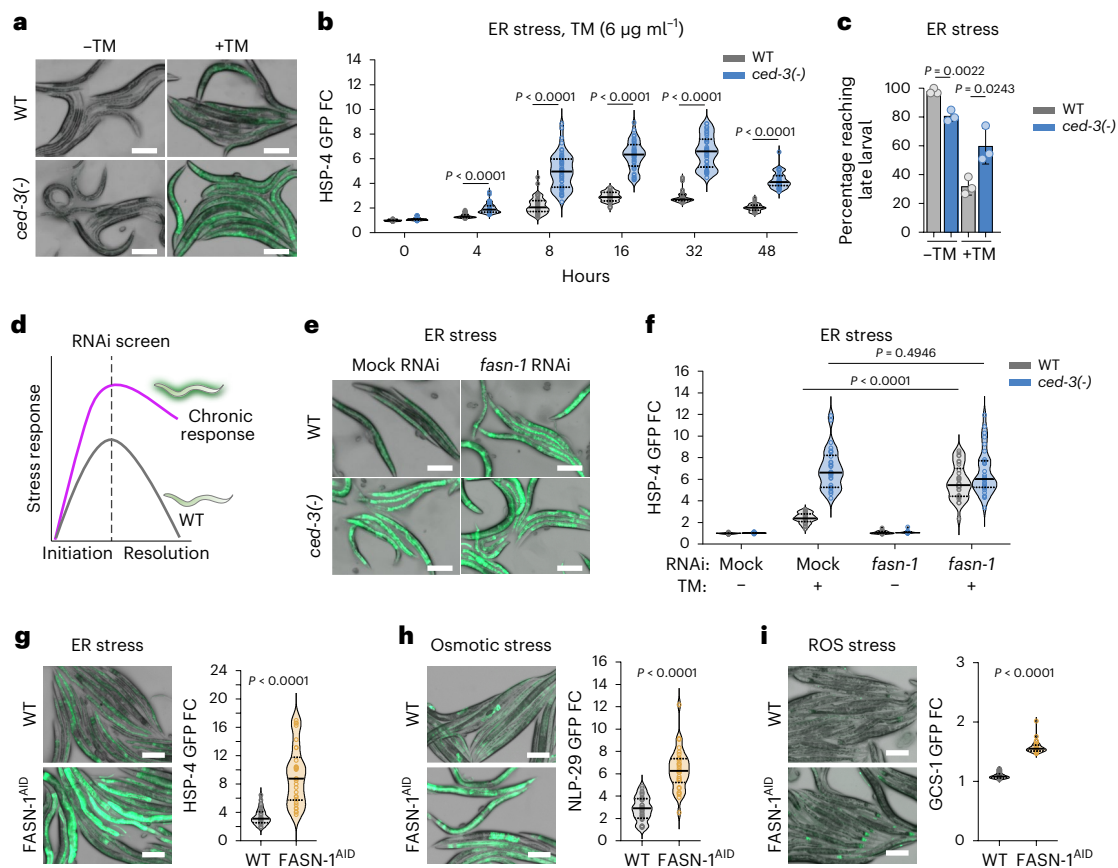
Fig. 1 | Caspase and FASN limit chronic pan-stress responses. a,b, Expression (**a**) and quantification (**b**) of intestinal ER stress reporter HSP-4p::GFP (Hsp70 member 5) with tunicamycin (TM) treatment to induce ER stress. WT, wild type. **c**, Quantification of animals escaping larval arrest with TM treatment. **d**–**f**, Targeted RNAi screen for chronic stress response factors (**d**) reveals that *fasn-1* acts like *ced-3* to limit stress response in HSP-4p::GFP expression (**e**) and quantification (**f**). **g**–**i**, Eliminating FASN-1 protein using AID also induces expression of stress reporters under ER (**g**), osmotic (**h**) and ROS (**i**) stresses by TM, sodium chloride and paraquat. Scale bar, 200 μm (**a**,**e**,**g**–**i**). Each circle represents one animal (**b**,**f**–**i**). Mean pixel intensity of each animal was normalized to mean value of WT at 0 h (no stress) and plotted as fold change (FC). Violin plots show median (solid line) with quartiles (dashed line). For **b**, 8 h, $n = 50$; 16, 32 and 48 h, $n = 40$. Mean ± s.d., $n = 3$ biological replicates (**c**). $n = 30$ animals for each time point (**f**–**i**). *P* values were calculated using a two-tailed Mann–Whitney *U*-test (**b**,**f**–**i**) and unpaired two-tailed *t*-test (**c**).

fasn-1(D/E) mutants. Notably, we did not observe any quantitative accumulation of FASN-1 cleavage fragments in *C. elegans* in the absence or presence of stressors (Extended Data Fig. 4h). These results suggest the possibility that only a small fraction of this highly abundant protein is cleaved by CED-3 in vivo.

We then tested the impact of *fasn-1(D/E)* on stress response. Similar to the *ced-3(-)* null mutant, the *fasn-1(D/E)* mutant had upregulated HSP-4p::GFP in response to tunicamycin (ER stress, Fig. 2f). This enhanced upregulation was equivalent to *ced-3(-)* (Extended Data Fig. 5a,b) and was confirmed with an independent second *fasn-1(D/E)* CRISPR mutant (Extended Data Fig. 5c). The *fasn-1(D/E)* mutant had enhanced survival comparable to *ced-3(-)* mutants (Extended Data Fig. 5d).

We next sought to test whether the *fasn-1(D/E)* mutant would have similar persistent phenotypes with other stressors. Analogous to the heightened ER stress response, the *fasn-1(D/E)* had dramatically enhanced induction of markers for both osmotic stress (NLP-29p::GFP) and ROS stress (GCS-1p::GFP) equivalent to *ced-3(-)* when challenged with high salt and paraquat, respectively (osmotic and ROS stresses; Fig. 2f and Extended Data Fig. 5e–j).

Altogether, these data suggest that CED-3 cleaves FASN-1 at the Asp1593 residue to limit pan-stress responsiveness in vivo. Because failure of cleavage caused by the *fasn-1(D/E)* mutation phenocopied the loss of caspase activity seen with the *ced-3(-)* mutant, we concluded

that a low level of caspase cleavage activates a distinct function of FASN to limit a pan-stress response.

FASN cleavage does not impact palmitate synthesis

The saturated fatty acid palmitate (C16) is the major end product of all metazoan FASN enzymes[2]. To test whether *ced-3(-)* and *fasn-1(D/E)* mutations have compromised palmitate synthesis, we performed metabolic labelling with D_2O to monitor fatty acid synthesis. We found no significant alterations in palmitate synthesis (Fig. 2g) or palmitoleate synthesis (Extended Data Fig. 5k) for *ced-3(-)* or *fasn-1(D/E)* mutants with or without ER stress.

To further confirm that the enhanced stress responsiveness of *ced-3(-)* and *fasn-1(D/E)* mutants was not due to a fatty acid deficiency, we supplemented animals with palmitate under ER stress and found that palmitate supplementation did not reduce the heightened HSP-4p::GFP induction in *ced-3(-)* null animals or *fasn-1(D/E)* cleavage-resistant mutants (Fig. 2h). In contrast, extra palmitate enhanced HSP-4p::GFP induction in wild-type, *ced-3(-)* and *fasn-1(D/E)* animals (Fig. 2h). Altogether, these results indicate that the stress-resolution function of cleaved FASN is independent of palmitate synthesis.

FASN cleavage by caspase impacts redox metabolism

To reveal the metabolic impact of CED-3 caspase on FASN-1, we used untargeted metabolomics in *C. elegans* to analyse the profiles of
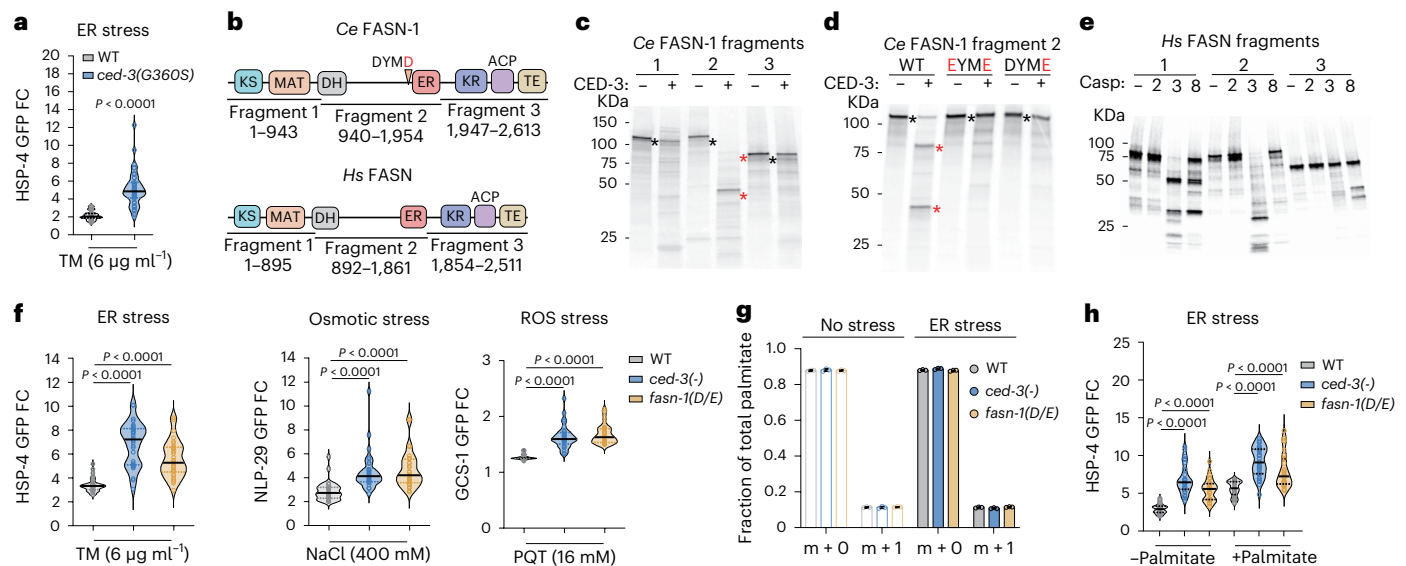
Fig. 2 | FASN activated by caspase cleavage limits pan-stress responses independent of palmitate synthesis. a, Expression of HSP-4p::GFP by caspase active-site mutation G360S. **b**, Highly conserved FASN domains and fragments used for in vitro caspase cleavage analyses. Enzymatic domains indicated with square boxes. *Ce*, *C. elegans*; *Hs*, *H. sapiens*. **c**,**d**, CED-3 in vitro cleavage of ^{35}S-labelled *C. elegans* FASN-1 fragments (**c**), the DYMD to DYME mutation (D/E) in fragment 2 blocks CED-3 cleavage (**d**). Red asterisks indicate cleaved products; black asterisks indicate full-length molecules. **e**, Conserved cleavage. ^{35}S-labelled human FASN is also cleaved in fragment 2 by caspase-3 producing a stable CTF similar to *C. elegans*. Casp, caspase-2, caspase-3 and caspase-8 as indicated for each lane. **f**, Cleavage-resistant *fasn-1(D/E) C. elegans* mutant phenocopies *ced-3(-)* mutant for enhanced inductions of ER, Osmotic and ROS stress reporters.

g, Measurement of palmitate synthesis using 50% deuterated water (D_2O) labelling for 16 h in the presence or absence of ER stress. m + 0, unlabelled palmitate; m + 1, deuterium-labelled palmitate representing newly synthesized palmitate. *n* = 3 biological replicates for each. Mean ± s.d. **h**, HSP-4p::GFP expression under ER stress with palmitate supplementation. Each circle represents one animal (**a**,**f**,**h**). Mean pixel intensity of each animal was normalized to mean value of WT without stress and plotted as FC. Violin plots show median (solid line) with quartiles (dashed line). For **a**, *n* = 40 animals for each genotype. *n* = 30 animals for each condition (**f**,**h**). *P* values were calculated using a two-tailed Mann–Whitney *U*-test. Cleavage assays (**c**–**e**) were repeated twice independently with similar results.

wild-type, *ced-3(-)* and *fasn-1(D/E)* strains in normal and stress conditions (Supplementary Data 1). When comparing *ced-3(-)* to wild-type, we found that 296 metabolites were significantly altered in the absence of stress (Fig. 3a). Additionally, when comparing *fasn-1(D/E)* to wild-type, we found that 242 metabolites were significantly altered (Fig. 3a). Of the 193 metabolites commonly altered in both mutants, 191 were changed in the same direction (Fig. 3b). Using Pearson's analysis, we also showed a strong positive correlation between *ced-3(-)* and *fasn-1(D/E)* (Extended Data Fig. 6a). Thus, *fasn-1(D/E)* shows 65% of the metabolic changes seen in *ced-3(-)* mutant before stress, reflecting a substantial common subset of metabolic alterations in both mutants.

To understand the variation for all detected metabolites, we used principal component analysis (PCA). Most of the variability was well represented in the first two principal components for each of the treatment conditions (Extended Data Fig. 6b). We found that the biggest variance in metabolites (PC1) corresponded to stress treatments, including ER (Fig. 3c), osmotic (Fig. 3d) and ROS stressors (Fig. 3e). The second largest variance represented by the PC2 axes corresponded to the different genotypes in the absence of stress. PC2 showed that the *ced-3(-)* and *fasn-1(D/E)* mutants clustered closer to each other (open circles, Fig. 3c–e), suggesting that the metabolic profiles of these two mutants are more similar to each other compared to the wild type. Notably, the dispersion among the genotypes on PC2 axes collapsed upon stress treatment (closed circles, PC2 axes; Fig. 3c–e). The clustering of wild-type with the mutants upon stress treatments suggests a subset of metabolites already altered in *ced-3(-)* and *fasn-1(D/E)* that normally occurs during the stress response.

Using enrichment analysis of metabolites altered in *ced-3(-)* or *fasn-1(D/E)* mutants, we found a significant enrichment for redox adaptations for both mutants in the absence of stress (Fig. 3f). Most homocysteine and glutathione metabolites detected are depleted

in both *ced-3(-)* and *fasn-1(D/E)* mutants in the absence of stress (no stress; Fig. 3g). Of note, the same depletion pattern was observed for wild-type animals under ER and osmotic stress conditions. ROS stress had a somewhat different pattern compared to the other two stressors but still resulted in an overall reduction of the cysteine pool (Fig. 3g). The glutathione pathway modulates cellular redox to mitigate stress responses. Unlike other stressors, ROS stress directly impacts cellular redox and paraquat detoxification directly modulates this pathway.

To further verify the alteration in redox metabolism, we used the Grx1-roGFP2 construct previously established to reflect the ratio of oxidized to reduced glutathione[12,13]. We found that *ced-3(-)* and *fasn-1(D/E)* mutants both have an increased ratio of oxidized to reduced glutathione in the absence of stress compared to wild-type (Extended Data Fig. 6c).

We also analysed other enriched pathways for *ced-3(-)* and *fasn-1(D/E)*, including carnitine and β-alanine pathways, and found that *ced-3(-)* and *fasn-1(D/E)* both showed most metabolites in those pathways decreased before stress but these alterations did not reflect the changes seen during stress (Extended Data Fig. 6d,e). Altogether, the metabolomic analyses revealed that both *ced-3(-)* null and the *fasn-1(D/E)* mutants had significant alterations in redox metabolism that resembles a stress-responsive state before encounter of a stressor.

Cell redox modulates caspase activity in stress

As a cys protease, caspases can be inhibited by oxidizing species[14] and highly oxidizing environments can even suppress caspase-mediated apoptosis[15,16]. To assess the relative alteration in caspase cysteine oxidation in cells as a result of exposure to oxidative stress, we treated primary mouse osteoblasts with hydrogen peroxide overnight. To enrich oxidized cysteine residues, we used the DCP-Bio1 probe that forms adducts with singly-oxidized cysteines (cysteine sulfenic acid).

We observed more than a threefold increase in oxidized caspase-3 cysteine residues when treated with the oxidizing agent hydrogen peroxide compared to vehicle-treated cells (Fig. 3h) without affecting caspase-3 protein levels (Extended Data Fig. 6f). These findings suggest that caspase cysteine residues are sensitive to cellular redox conditions. We next considered whether oxidized cellular environments caused by other stressors would impact caspase activity.

ER stress both results from the accumulation of (and itself generates) ROS[17,18]. To test whether cellular oxidation is induced by ER stress, we examined the ratio of oxidized to reduced glutathione metabolites and observed an increased ratio in oxidized to reduced glutathione in *C. elegans* (Extended Data Fig. 6g), suggesting a more-oxidative cellular environment under ER stress. Because caspase auto-processing requires enzymatic activity of caspase, we tested how ER stress affects CED-3 auto-processing in *C. elegans*. We found that overnight ER stress treatment resulted in diminished CED-3 auto-processing in vivo (Fig. 3i). ER stress increased the accumulation of full-length CED-3 protein that corresponded to decreased accumulations of both the p32 and p15 processed subunits (Fig. 3i). This observation indicates that CED-3 has diminished proteolytic capability under ER stress.

In mammals, liver is a tissue enriched for FASN expression[19,20] and fasting induces oxidative stress on the liver[21,22]. Therefore, we analysed the effect of fasting on FASN and caspase expression in male mouse liver. During the well-fed state, we found FASN processing along with the presence of active caspase-3, whereas both were absent during prolonged fasting (Fig. 3j). Altogether, these findings indicate that caspase cysteine oxidation and subsequent inhibition of caspase activity can occur during stress conditions. The decrease of caspase activity would thereby lead to further depletion of GSH redox buffer causing a heightened stress response similar to the *ced-3(-)* mutation (Fig. 3k).

To further test whether modulating cellular redox status directly impacts CED-3 caspase-dependent stress responsiveness, we supplemented *ced-3(-)* animals with antioxidants *N*-acetylcysteine (NAC; Fig. 3l and Extended Data Fig. 7a,b) or L-carnosine (Fig. 3m and Extended Data Fig. 7c,d) under ER stress conditions. We found that both antioxidant supplements significantly reduced the heightened ER stress response in *ced-3(-)* mutants. These findings suggest that the CED-3 caspase-mediated stress response can be reversed by increasing the cellular reductive capacity.

Conversely, we then considered how organismal stress response would be impacted by shifting the redox state toward an oxidative profile. Lipid peroxidation occurs as a result of oxidative bursts and elevated cellular ROS results in accumulation of lipid-derived reactive aldehydes such as malondialdehyde (MDA). When supplementing animals with MDA, we found that wild-type animals had increased response to ER stress similar to *ced-3(-)* mutants without MDA (Fig. 3n and Extended Data Fig. 7e,f). Moreover, MDA did not further increase the elevated response of *ced-3(-)* mutants (Fig. 3o). To eliminate the

possibility of reaching the reporter detection limit, we repeated the same assay at lower concentrations of tunicamycin and found that the ER stress reporter in *ced-3(-)* mutants was not further enhanced by MDA even at low TM concentrations well below maximal responsiveness (Extended Data Fig. 7g,h). This result indicates that elevated cellular oxidative environment augments stress response and loss of CED-3 caspase mimics an elevated oxidative cellular environment. Because *ced-3(-)* null and the cleavage-resistant *fasn-1(D/E)* mutants both had increased amplitude in stress responses, we concluded that CED-3 proteolytic activity may be redox sensitive to modulate the magnitude of response, suggesting the possibility of FASN cleavage as a signal to scale down stress response.

FASN-CTF attenuates pan-stress response

To understand the functional outcome of CED-3 cleavage on FASN in vivo, we used CRISPR mutagenesis to insert either the N- or C-terminal cleaved fragment as a single extra copy in *C. elegans* (Fig. 4a). The FASN N-terminal fragment (NTF) generated a spectrum of processing bands, whereas the CTF made one stable product (Fig. 4a). Further analysis of the FASN-NTF revealed that the linker region at the end of the NTF likely contains a degron when exposed by proteolytic cleavage (Extended Data Fig. 8a,b).

To analyse the impact of both FASN NTFs and CTFs in stress resolution, we tested the effects of expressing either fragment in *ced-3(-)* null mutants upon stress (Fig. 4b,c). We found that the expression of FASN-CTF is sufficient to resolve the enhanced stress responsiveness of the *ced-3(-)* mutant, whereas the NTF is not (Fig. 4b,c). Moreover, tissue-specific expression of FASN-CTF in either the intestine or muscle (Extended Data Fig. 8c) also decreased the heightened induction of the intestinal HSP-4p::GFP of the *ced-3(-)* mutant (Fig. 4d,e). Therefore, we concluded that FASN-CTF can function cell non-autonomously to decrease the stress response.

Because FASN is an essential gene for de novo fatty acid synthesis and loss of FASN-1 causes developmental arrest in *C. elegans*[5,23], we wanted to determine whether the FASN-CTF works in a dominant negative manner to inhibit full-length FASN de novo fatty acid synthesis. As loss of FASN function compromises development, we measured the growth rate of animals with and without CTF expression to assess the impact on development. We found that animals expressing FASN-CTF had no growth delay compared to animals not expressing the CTF (Fig. 4f). These findings suggest that the FASN-CTF functions to decrease stress response without compromising essential de novo fatty acid synthesis function of FASN during development.

FASN-CTF promotes anti-inflammatory profile

To further investigate the impact of FASN-CTF on gene expression, we performed mRNA-seq analysis (Supplementary Data 2). We found that with ER stress, expressing the CTF in *ced-3(-)* decreased expression


Fig. 3 | Interplay of cellular redox state and FASN cleavage determines stress responsiveness. a,b, Alterations of metabolites in *ced-3(-)* and *fasn-1(D/E)* animals compared to WT in the absence of stress from untargeted metabolomics. Untargeted metabolomics with $P < 0.05$ as cutoff revealed 193 overlapping metabolites (**a**) shown in heat map (**b**) in *ced-3(-)* and *fasn-1(D/E)*. $n = 6$ biological replicates. **c**–**e**, PCA of untargeted metabolites for WT, *ced-3(-)* and *fasn-1(D/E)* animals with ER (**c**), osmotic (**d**) and ROS (**e**) stressors. **f**, Metabolite enrichment analyses for *ced-3(-)* null and *fasn-1(D/E)* mutants compared to WT using MetaboAnalyst with the Small Molecule Pathway Database (SMPDB). False discovery rate (FDR) < 0.1. Input list from metabolites shown in **a** with $P < 0.05$, *ced-3(-)* 296 and *fasn-1(D/E)* 242 metabolites. **g**, Heat map of detected metabolites in glutathione pathway. $\log_2 FC$ relative to mean value of WT no stress. **a**–**g**, $n = 6$ biological replicates. P values calculated using an unpaired two-tailed *t*-test (**a,b,g**) or one-tailed Fisher's exact test (**f**). **h**, Caspase-3 cysteine oxidation in primary mouse calvarial osteoblasts (cOBs) using DCP-Bio1 IP MS. Average abundance of caspase-3-oxidized cysteine treated with vehicle was set

to 1.0. Total caspase-3 protein in lysate (Extended Data Fig. 6f). Veh, water. $n = 3$ biological replicates. Mean ± s.d. **i**, CED-3 auto-processing monitored by western blot of endogenous CED-3 with a C-terminal HA tag under ER stress. CED-3 auto-processing with ER stress was repeated independently twice with similar results. **j**, Western blot of liver extracts from well-fed or 36-h-fasted male mice showing processing of FASN and cleaved caspase-3. $n = 3$ male mice for each condition. **k**, Diagram of caspase cys active site as a function of oxidative state and impact on stress responsiveness. **l,m**, Expression of HSP-4p::GFP under ER stress with NAC (**l**) or carnosine (**m**) antioxidant supplementation in *ced-3(-)* animals. **n,o**, Induction of HSP-4p::GFP under ER stress with oxidized lipid metabolite MDA supplementation in WT (**n**) and *ced-3(-)* (**o**) animals. Each circle represents one animal. Mean pixel intensity of each animal normalized to mean value of WT without stress and plotted as FC. Violin plots show median (solid line) with quartiles (dashed line). P values were calculated using an unpaired, two-tailed *t*-test. $n = 3$ biological replicates (**h**) or two-tailed Mann–Whitney *U*-test. $n = 30$ animals for each time point (**l**–**o**).

of genes enriched for pathogen defence and IRE1-mediated unfolded protein response (UPR) (Fig. 4g and Extended Data Fig. 8d,e). We also saw mixed alterations in genes enriched for cytochrome P450 and lipid metabolism. Genes in pathogen defence and UPR were almost all downregulated by FASN-CTF (Fig. 4g and Extended Data Fig. 8d,e). Finding suppression of immune and stress-responsive

gene expression suggests a strong anti-inflammatory-type function for the FASN-CTF.

To overcome limitations of BLAST-based Gene Ontology enrichment, we also used the WormCat gene set enrichment analysis tool to analyse these genes in more detail[24]. WormCat also identified pathogen response, heat stress, cellular detoxification and lipid metabolism
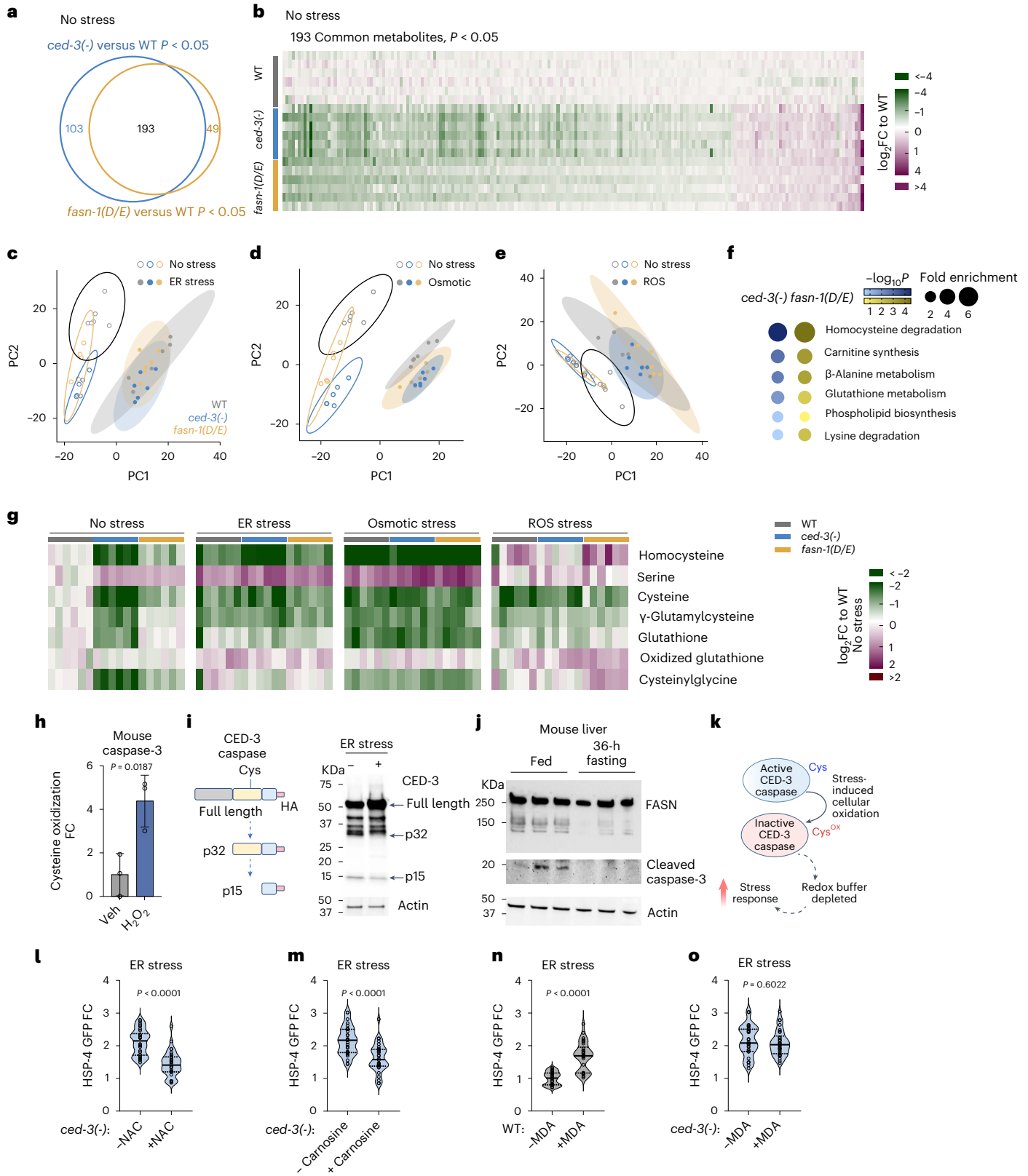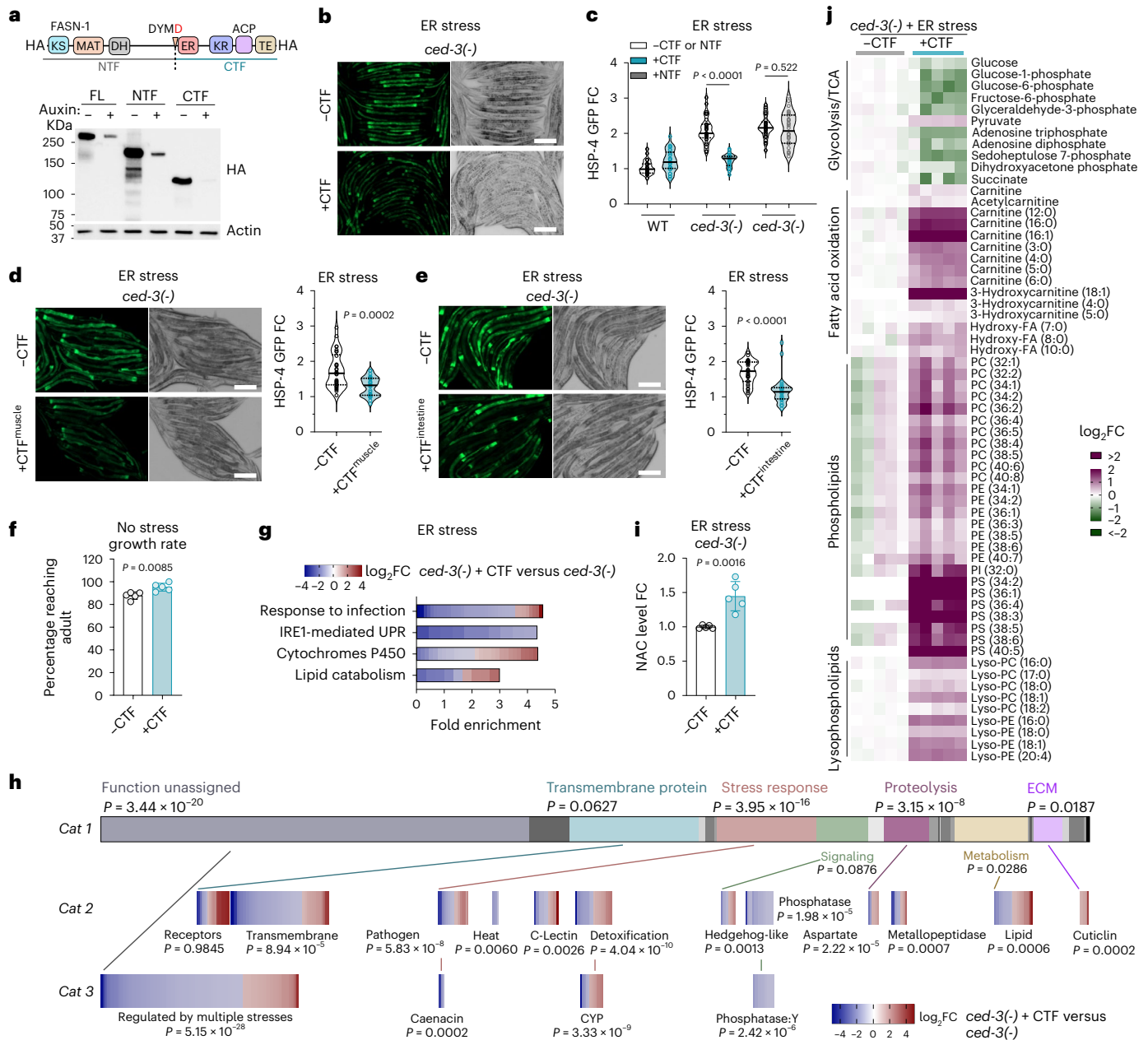
Fig. 4 | FASN-CTF diminishes chronically elevated stress-responsive gene expression and metabolic programs. a, Western blot showing in vivo stabilities of FASN-NTF and CTF. Auxin-controlled endogenous FASN-1 (FL) or a single-copy transgene expressing either NTF or CTF all contain an HA tag for detection. Western blot for stability of FASN fragments was repeated twice independently with similar results. **b,c**, HSP-4p::GFP expression (**b**) and quantification (**c**) under ER stress with expression of FASN-CTF or NTF in *ced-3(-)*. *n* = 30 animals. **d,e**, HSP-4p::GFP induction under ER stress in *ced-3(-)* animals with expression of FASN-CTF only in muscle (**d**) or only in intestine (**e**). *n* = 30 animals (**d,e**). Scale bar, 200 μm (**b,d,e**). **f**, Growth rate of animals with and without expression of FASN-CTF. *n* = 5 biological replicates with total of *n* = 441 (−CTF) and *n* = 303 (+CTF) animals were assayed. Mean ± s.d. **g,h**, Impact of FASN-CTF on *ced-3(-)* mutant for alterations in gene expression under ER stress using the gene set analysis tool in WormBase

(wormbase.org/tools/enrichment/tea/tea.cgi) (**g**) and WormCat (wormcat. com/) (**h**). Heat maps (**g,h**) show mRNA log$_2$FC of *ced-3(-)* mutant expressing CTF compared to *ced-3(-)* with no CTF expression. *n* = 3 biological replicates. FDR < 0.1 and absolute value of log$_2$FC > 1 were thresholds for enrichment analysis (**g,h**). **i**, NAC level in *ced-3(-)* with and without CTF expression. *n* = 5 biological replicates. Mean ± s.d. **j**, Impact of FASN-CTF expression on *ced-3(-)* mutant for selected metabolites under ER stress. Heat map shows log$_2$FC of *ced-3(-)* mutant expressing CTF compared to *ced-3(-)* with no CTF expression. *n* = 5 biological replicates. FA, fatty acid; PC, phosphatidylcholine; PE, phosphatidylethanolamine; PI, phosphatidylinositol; PS, phosphatidylserine; Lyso-PC, lysophosphatidylcholine; Lyso-PE, lysophosphatidylethanolamine; TCA, tricarboxylic acid. *P* values were calculated using an unpaired two-tailed *t*-test (**f,i**), two-tailed Mann–Whitney *U*-test (**c–e**) or one-tailed Fisher's exact test (**h**).

as highly enriched (Fig. 4h). In addition, the new analysis identified an enrichment of a large set of genes with no functional assignment but regulated by multiple stresses (Fig. 4h). More than 70% of these genes were downregulated with the expression of FASN-CTF. Moreover, WormCat analysis revealed new enrichment for transmembrane

proteins, proteolysis factors and tyrosine phosphatase, suggesting a possible role of FASN-CTF in cellular remodeling and signaling.

We also analysed the metabolic impact of expressing FASN-CTF on *ced-3(-)* and wild-type animals under ER stress using targeted metabolomics (Supplementary Data 3 and Extended Data Fig. 8f,g).
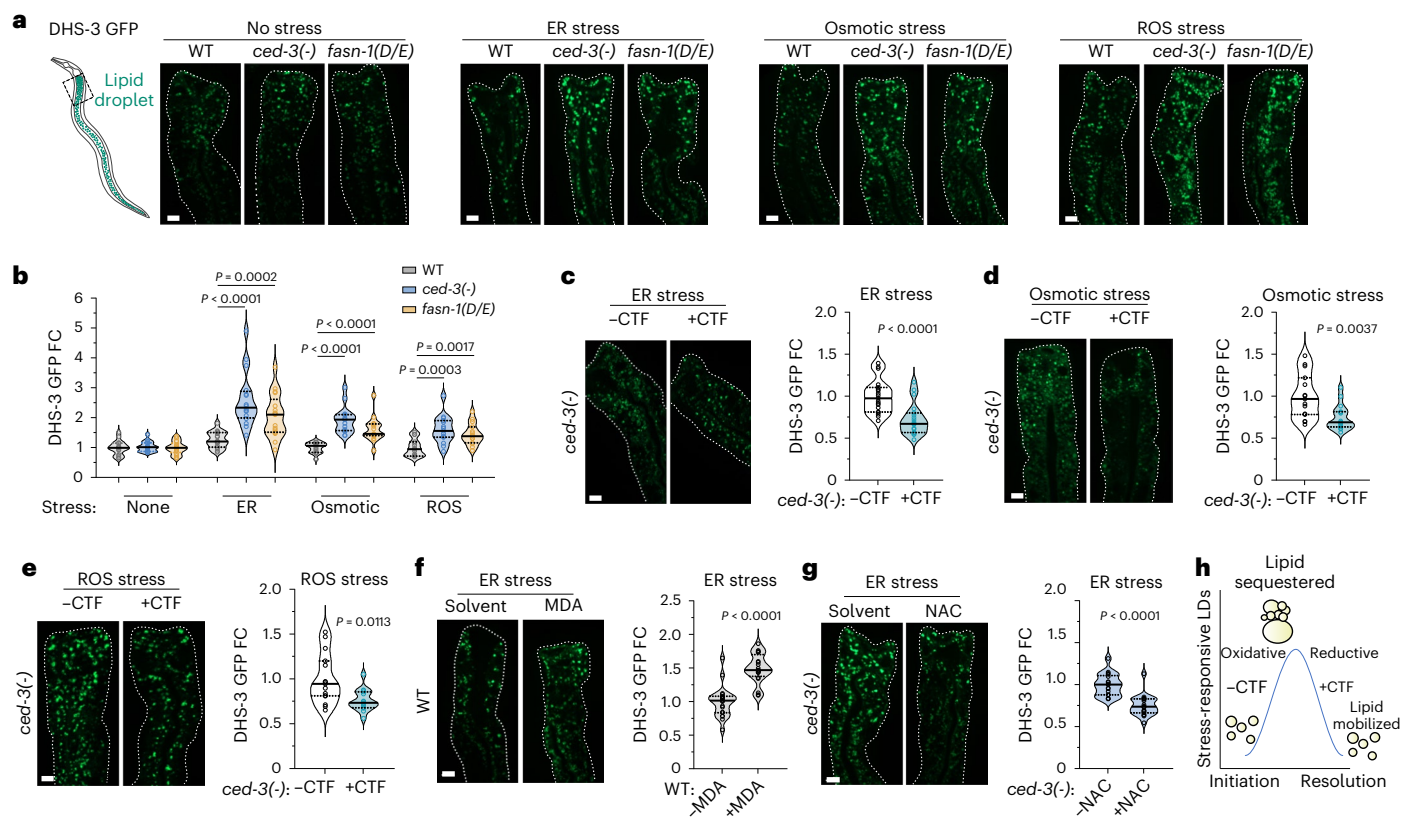
Fig. 5 | FASN-CTF resolves stress-induced lipid droplets. a,b, Lipid droplets visualized (**a**) and quantified (**b**) in the same region of intestine by DHS-3::GFP marker intensity under ER, osmotic and ROS stresses. $n = 15$ for osmotic and ROS, $n = 16$ for no treatment and ER stress except *fasn-1(D/E)* $n = 17$ animals per condition. **c–e,** Lipid droplets with expression of FASN-CTF in *ced-3(-)* mutant animals under ER stress, $n = 19$ animals (**c**), osmotic stress, $n = 15$ animals (**d**) and ROS stress, $n = 15$ animals (**e**). **f,g,** Lipid droplets with supplementation of MDA in WT animals (**f**) and NAC in *ced-3(-)* animals (**g**) under ER stress. $n = 19$ animals on control and 20 animals on MDA. $n = 17$ animals on control and 19 animals on NAC. **h,** Diagram illustrating relationship of lipid droplet (LD) accumulation with CTF expression and cellular oxidative status. Scale bar, 10 µm (**a,c–g**). *P* values were calculated using a two-tailed Mann–Whitney *U*-test (**b–g**).

Of note, we found elevated NAC antioxidant with FASN-CTF expression in *ced-3(-)* under ER stress but not in wild-type animals (Fig. 4i and Extended Data Fig. 8h). This finding was consistent with our observation that supplementing NAC reduces the heightened ER stress response in *ced-3(-)* null mutants but not wild-type animals (Fig. 3l and Extended Data Fig. 7a).

We also found that *ced-3(-)* null mutants with ectopic expression of FASN-CTF had altered enrichments for metabolites in multiple energy production pathways (Extended Data Fig. 8i). Specifically, when expressing FASN-CTF in *ced-3(-)* null mutants, of metabolites tested, most of the glycolysis and tricarboxylic acid cycle pathway metabolites were decreased (Fig. 4j). Conversely, almost all the carnitine species, hydroxy-fatty acids and phospholipids tested were increased with FASN-CTF expression (Fig. 4j), suggesting the possibility of altered fatty acid oxidation. With intact CED-3 function in wild-type animals, the FASN-CTF had a much less-pronounced impact on the metabolic profile with a mild increase in carnitine metabolites (Extended Data Fig. 8j), suggesting that the CTF-mediated metabolic changes suppress the lack of CED-3 function.

To address the possibility of altered respiration, we tested the impact of FASN-CTF on oxygen consumption rate (OCR) but did not observe any obvious alteration of *ced-3(-)* with or without CTF expression (Extended Data Fig. 8k), suggesting that substrate switching rather than altered metabolic rates may be more predominate. Altogether, we found that expressing FASN-CTF attenuates stress-responsive gene programs, elevates reducing metabolites and, notably, shifts metabolic substrate composition with elevated soluble lipids.

FASN-CTF resolves stress-induced lipid droplets

Lipid droplets serve as readouts of stress responses as they play essential roles in mitigating stress responses, integrating lipid metabolism with energy homeostasis, supporting proteostasis during stress responses, sequestering reactive oxidizing species and supporting immune signaling[25–27]. To observe intestine-specific lipid droplets, we used the DHS-3::GFP fusion protein as a previously established marker in *C. elegans*[28]. Without stress treatment, *ced-3(-)* null and *fasn-1(D/E)* mutants had no effect on basal lipid droplet intensity as visualized by DHS-3::GFP (no stress; Fig. 5a). With challenges from ER, osmotic and ROS stress, *ced-3(-)* and *fasn-1(D/E)* mutants had a marked increase in lipid droplet intensity (Fig. 5a,b) but had no impact on the DHS-3::GFP protein levels (Extended Data Fig. 9a), suggesting increased accumulation of lipid droplets in *ced-3(-)* and *fasn-1(D/E)* mutants with stress treatments.

We next tested whether expressing FASN-CTF would impact the lipid droplet dynamics of *ced-3(-)* mutants. We found that the FASN-CTF was able to ameliorate the heightened lipid droplet accumulation in *ced-3(-)* mutants with ER (Fig. 5c), osmotic (Fig. 5d) and ROS stressors (Fig. 5e). When expressing FASN-CTF in wild-type animals, there were no differences in lipid droplets with ER, osmotic or ROS stressors (Extended Data Fig. 9b–d). This was expected, given that wild-type animals have functional CED-3 and FASN-1.

Given the ability of the FASN-CTF to promote cellular reductive capacity, we further tested how lipid droplet dynamics were affected by altering cellular redox conditions. We found that supplementing wild-type animals with the lipid aldehyde metabolite MDA enhances
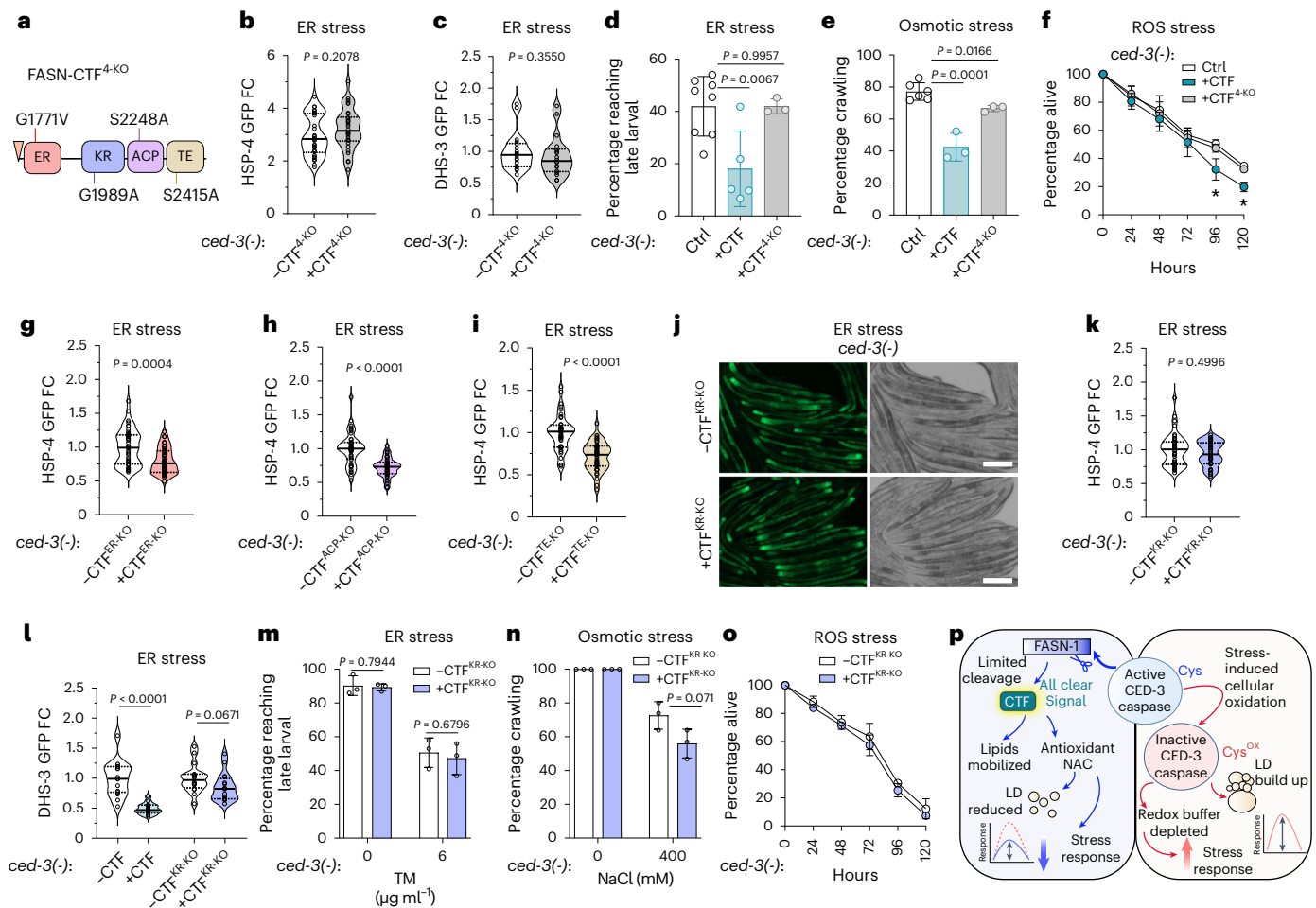
Fig. 6 | Impact of FASN-CTF enzymatic activity on pan-stress resolution and fitness. a, Diagram of FASN-CTF with four point mutations that inactivate the four conserved enzymatic domains (FASN-CTF[4-KO]). **b**, Induction of ER stress marker HSP-4p::GFP with expression of FASN-CTF[4-KO] under ER stress in *ced-3(-)* mutant animals. *n* = 30 animals. **c**, Induction of LD marker DHS-3p::GFP with expression of FASN-CTF[4-KO] under ER stress in *ced-3(-)* mutant animals. *n* = 18 animals. **d–f**, Artificially driving FASN-CTF expression during stress compromises survival. Developmental impact with either FASN-CTF or FASN-CTF[4-KO] measured by developmental rate, motility and survival of *ced-3(-)* mutant animals under ER (**d**), osmotic (**e**) and ROS (**f**) stress conditions. *n* = 5 for CTF, *n* = 3 for CTF[4-KO] and *n* = 8 for no CTF (Ctrl) biological replicates (**d**). Mean ± s.d. *n* = 3 for CTF and CTF[4-KO] and *n* = 6 for no CTF biological replicates (**e**,**f**). Mean ± s.d. **g–i**, Quantification of HSP-4p::GFP with expression of FASN-CTF[ER-KO] (enoyl reductase domain mutant) (**g**), FASN-CTF[ACP-KO] (ACP domain mutant) (**h**) and

FASN-CTF[TE-KO] (TE domain mutant) (**i**) under ER stress in *ced-3(-)* mutant animals. *n* = 40 animals each. **j**,**k**, Image (**j**) and quantification (**k**) of HSP-4p::GFP with expression of FASN-CTF[KR-KO] (KR domain mutant) under ER stress in *ced-3(-)* mutant animals. Scale bar, 200 µm. *n* = 40 animals each. **l**, Induction of LD marker DHS-3p::GFP with expression of FASN-CTF[KR-KO] under ER stress in *ced-3(-)* mutant animals. *n* = 14 *ced-3(-)* with CTF, *n* = 15 *ced-3(-)* without CTF and *ced-3(-)* with or without CTF[4-KO], *n* = 16 animals. **m–o**, Developmental impact with FASN-CTF[KR-KO] measured by developmental rate, motility and survival of *ced-3(-)* mutant animals under ER (**m**), osmotic (**n**) and ROS (**o**) stress conditions. *n* = 3 biological replicates (**m–o**). Mean ± s.d. *P* values were obtained by two-tailed Mann–Whitney *U*-test (**b**,**c**,**g–i**,**k**,**l**) and unpaired, two-tailed *t*-test (**d–f**,**m–o**). **p**, Diagram illustrating the model of caspase CED-3 acting as stress sensor, generating FASN-CTF through cleavage of FASN to attenuate the stress response.

lipid droplet accumulation under ER stress (Fig. 5f), whereas supplementation with the antioxidant NAC ameliorated lipid droplet accumulation in *ced-3(-)* mutants (Fig. 5g). These findings indicate that expressing FASN-CTF had similar effects on lipid droplet dynamics as restoring cellular redox (Fig. 5h).

FASN-CTF KR activity signals stress resolution

Previous work identified point mutations that disrupt mammalian FASN enzymatic activity[1]. We introduced a transgene of FASN-CTF with point mutations of the highly conserved residues to inactivate each of the four domains in the FASN-CTF and referred to as FASN-CTF[4-KO] (Fig. 6a). These residues were identified by homology to the human FASN (Extended Data Fig. 9e). FASN-CTF and FASN-CTF[4-KO] were expressed at similar levels and were both responsive to auxin-induced degradation (Extended Data Fig. 9f). Analogous to FASN-CTF,

expression of FASN-CTF[4-KO] did not delay development under normal conditions, suggesting that it also does not impact endogenous FASN-1 function (Extended Data Fig. 9g). In contrast to FASN-CTF, expression of FASN-CTF[4-KO] did not suppress the ER stress response as visualized by continued expression of HSP-4p::GFP (Fig. 6b and Extended Data Fig. 9h). Additionally, FASN-CTF[4-KO] also did not ameliorate heightened lipid droplet accumulation (Fig. 6c and Extended Data Fig. 9i).

To distinguish whether the FASN-CTF functions more as an effector to mitigate stress or more as a signal to scale down stress responses, we assayed developmental progression under ER stress. We found that expression of FASN-CTF led to more stalled development for the *ced-3(-)* mutants in the presence of ER stress (+CTF; Fig. 6d). In contrast, FASN-CTF[4-KO] behaved similar to *ced-3(-)* mutants (+CTF[4-KO]; Fig. 6d). Similarly, expression of FASN-CTF led to less motility under osmotic stress (Fig. 6e) and fewer survivors under ROS stress (Fig. 6f). Because

expressing FASN-CTF decreased overall fitness of *ced-3(-)* mutants under diverse stress conditions, we concluded that the presence of FASN-CTF before stress mitigation compromises survival as it provides a premature stress-resolution signal.

These results suggest that catalytic activity of FASN-CTF is required for its function in attenuation of the stress response. To distinguish whether all four CTF domains or a specific domain were required, we generated single mutants to disrupt each of the enzymatic activities, including the enoyl reductase, KR, ACP and TE domains (Extended Data Fig. 10a) as these were mutated in the combined CTF 4-KO construct (Extended Data Fig. 10a). We found that each of the single mutants was expressed to similar extents as wild-type CTF and degraded in an auxin-dependent manner similar to wild-type CTF (Extended Data Fig. 10b,c). Elimination of the enoyl reductase, ACP or TE activities individually still allowed for suppression of HSP-4p::GFP induction (Fig. 6g–i and Extended Data Fig. 10d,e); however, disruption of either the enoyl reductase and KR domains jointly (2KO) or the KR domain alone (KR-KO) each abrogated the CTF suppression of HSP-4p::GFP induction (Fig. 6j,k and Extended Data Fig. 10d,f). Moreover, the KR domain single mutant failed to suppress accumulated lipid droplets (Fig. 6l and Extended Data Fig. 10g). In contrast to wild-type CTF, there was also no difference for *ced-3(-)* mutants expressing the CTF KR-KO domain single mutant when challenged with ER stress (Fig. 6m), osmotic stress (Fig. 6n) or ROS stress (Fig. 6o). Altogether, our findings suggest that the KR domain is critical for the FASN-CTF stress-suppression function.

In conclusion, we propose that FASN-CTF is generated by caspase cleavage in a redox-dependent manner. Under stress conditions, a more-oxidative cellular environment renders CED-3 caspase less active, leading to depleted redox buffer, lipid droplet accumulation and an increased stress response. Once stress is mitigated, a less-oxidative cellular environment reactivates caspase and generates FASN-CTF through proteolytic cleavage of FASN. FASN-CTF functions as an 'all clear' signal to initiate a stress response attenuation program. As an all clear signal, FASN-CTF is sufficient to promote lipid mobilization and reduce lipid droplet accumulation as well as downregulate stress response genes. As a result, physiological adaptations are re-programmed for a non-stress state to support growth and homeostasis (Fig. 6p).

Discussion

In this study, we are proposing that FASN cleavage is a sensor that gauges a stress-free state. Under wild-type conditions, following restoration of redox balance, caspase is reactivated, allowing for cleavage and generation of FASN-CTF to downregulate the stress response (Fig. 6p). Thus, if FASN-CTF expression was forced without mitigating a stressor, this would provide an inappropriate downregulation of the stress response and would be detrimental to survival. Enhancing stress responsiveness improves survival during stressful states but is detrimental during stress-free conditions (chronic stress response). Conversely, diminishing a stress response prematurely would be detrimental without complete removal of the stressor (blunted stress response). Thus, organisms benefit from robust stress responses balanced with stress-sensing mechanisms.

Previous work analysing cell death factors, including *ced-3* caspase and *ced-4* Apaf, enhanced survival under stressful conditions through an unknown mechanism[4]. More recent work using a tamoxifen-induced ROS model demonstrated that the extent of lipid oxidative stress is modulated by the interplay of dietary fatty acids, host fatty acid metabolism and cell death pathways[29]. These findings suggest that innate adaptive mechanisms and host–diet interactions further alter the trajectory of stress responses. Moreover, that recent study also provided a scenario whereby, in response to an injury, some components, including oxidative status and cell death machinery, could themselves be entangled[29]. Additional recent findings show that ROS acting on dietary lipids compromises germ cell survival via ferroptosis and this can be alleviated by antioxidants[30]. Our present findings show an interplay of cellular redox and caspase cleavage of FASN in the determination of stress responsiveness.

Lipid biosynthesis itself has a notable function in activating stress responses. Compromised de novo fatty acid synthesis by mutation of *fasn-1* enhanced the expression of antimicrobial genes in *C. elegans*[23] and oxidative stress response genes in yeast[31]; however, lipid biosynthesis by FASN-1 was shown to be required to initiate the mitochondria-to-cytosolic stress response, triggering HSF-1 and DVE-1 transcriptional programs[32]. Moreover, FASN is required for diet-induced inflammatory signaling[33] as well as axonal regeneration following nerve injury[34]. These seemingly contradictory findings suggest a complex role for FASN in stress responses, which could be explained by the established lipid synthesis role as well as the signaling that we find.

Lipid droplets reflect an integrated readout of the stress response, protecting cells from excessive free lipids, sequestering toxic lipids, buffering ER stress by deposition of unfolded proteins and even serving as platforms for immune signaling[26]. Under stress, cells have a net increase in lipid droplets and their diminution is consistent with a diminished stress response. Previous studies have elegantly elucidated the regulation of lipid droplet formation and dynamics of turnover[28,35–40], yet many questions remain unanswered, particularly with regard to the order of events and which steps represent full or reversible commitment in lipid droplet formation, release and dissolution. Further, despite considerable work showing the protective effects of lipid droplet formation, recent work has shown that lipid droplets can also be toxic when formed in the wrong context, such as in the nucleus of certain cells[41]. In this study, we reveal heightened lipid droplet accumulation in *ced-3(-)* and *fasn-1(D/E)* mutants consistent with a chronic stress response phenotype. Further, the enhanced accumulation of droplets along with other stress markers was ameliorated in *ced-3(-)* mutants by expression of FASN-CTF. Although we do not know the mechanism of lipid droplet reduction, it represents a readout of stress resolution.

Alterations in lipid accumulation activate SKN-1 Nrf, which itself is critical in lipid homeostasis[42]. Redox-sensitive transcriptional programs are essential to initiate an antioxidant response that mitigates oxidative challenges[43,44]. Thus, a reversible sensor acting at the post-translational level would reinforce the dynamic sensing of stress responses, allowing for rapid sequestration of energy stores. Limiting lipid peroxidation is of paramount importance for cell survival during stress[45]. Thus, it is noteworthy that the fatty acid-synthesizing enzyme FASN would also have a stress-sensing function, signaling the all clear after stressful encounters have been attenuated. Additionally, a shift in redox is a general feature of many stressful and pathogenic states, making redox restoration coupled with lipid droplet dynamics an effective adaptive response for stress mitigation. Moreover, accurately gauging a response proportional to the challenge without mounting an excessive response allows cellular energy supplies to be conserved. Redox signaling is complex, in that the redox factors can take on multiple roles[46,47].

Efforts to map the cysteinome have revealed an array of oxidized cysteine species and complex roles of cysteine redox in signaling, gene expression, cellular growth and stress responses[48,49]. Depending on the oxidation state, multiple cysteine oxidation species are reversible[50,51]; however, some cysteine oxidation forms are irreversible[50,51]. Following redox resolution by mechanisms including SKN-1 Nrf transcriptional regulation[43,44,52], NADPH oxidase signaling[53] and subsequent sulfide production[54], cysteine redox balance is collectively restored and the caspase active-site cysteine would be reactivated and allow for normal lipid droplet dynamics. Therefore, caspase makes for an intriguing sensor of oxidation state where mitigation of ROS could restore activity and allow resumed proteolytic activity. Future work will need to delineate whether redox restoration alone is sufficient or whether other factors in addition to redox are also required to restore caspase activity

following stress responses in vivo. Either way, our findings show that caspase activity is altered by stress conditions.

Animals have evolved signaling mechanisms ranging from lipid-derived ligands to phosphorylation cascades to protein–protein interactions. In many cases, the signaling molecule or interaction responsible for these functions is present at minute levels, yet has potent roles as pro-development or stress-activating cues. Solving each of these elegant signaling mechanisms as multi-step cascades represented considerable effort with numerous studies. Our present findings reveal an unexpected role of FASN in detecting stress levels via a redox-sensitive, caspase-dependent proteolytic generation of the FASN-CTF. Of the four domains located in the CTF, we find that only the KR domain is essential for the stress-suppression function. The canonical activity of the KR enzyme family is to reduce acetoacetyl groups to hydroxyacyl groups in an NADP-dependent manner. Whether or not that is the relevant function in stress suppression will require significant future study. We find that generation of the FASN-CTF is a strong stress-resolution cue. Generation of the FASN-CTF can even be detrimental with forced expression of FASN-CTF without mitigation of the stressor. The duality of FASN as a biosynthetic enzyme and a generator of the FASN-CTF stress-resolution cue suggests that FASN may have a broader role as a signaling hub integrating basic metabolic demands and stress inputs.

Methods

Maintenance of *C. elegans* strains

All strains were maintained well fed at 20 °C for more than five generations before the experiments. Standard OP50 NGM plates were used unless otherwise indicated. RNAi clones were expressed in HT115 bacteria seeded on plates with 200 µg ml^{-1} ampicillin and 1 mM IPTG. For auxin treatments, 0.5 mM K-NAA auxin analogue (QJ-3105 Combi-Blocks) was used for each plate and animals were treated for the indicated times. Supplementary Table 1 lists all strains used in the study.

Stress treatment and metabolite supplementation

TM (T7765, Sigma-Aldrich) was dissolved in dimethylsulfoxide (DMSO) as a 5 mg ml^{-1} stock for ER stress. Sodium chloride (S7653, Sigma-Aldrich) was dissolved in H$_2$O as a 4 M stock for osmotic stress. Paraquat (856177, Sigma-Aldrich) was dissolved in H$_2$O as a 1 M stock for ROS stress. For metabolite supplementation, 20 mg ml^{-1} stock solutions were made for each of the following metabolites: sodium palmitate (P9767, Sigma-Aldrich, in 1% NP-40), NAC (A7250, Sigma-Aldrich, in DMSO), L-carnosine (C9625, Sigma-Aldrich, in H$_2$O), MDA (63287, Sigma-Aldrich, in H$_2$O) and tetrabutylammonium chloride (86870, Sigma-Aldrich, in H$_2$O).

To make NGM/TM agar plates with stressors or metabolite supplements, stock solution was diluted in H$_2$O to a final volume of 400 µl as a working solution. The working solution was spread on an empty NGM agar plate surface to make the indicated concentration. Bacteria OP50 or HT115 was seeded once the surface had dried. An equal volume of solvent was used as a control. All plates were made fresh before the stress test.

For HSP-4p::GFP, NLP-29p::GFP and GCS-1p::GFP reporter induction, the same number of animals (~300 animals) were placed on each NGM plate treated with individual stressors. All animals were incubated at 20 °C overnight or at the indicated time points before imaging.

For metabolite supplementation, synchronized late-L3 animals were placed on an NGM plate with individual metabolite supplementation or solvent control for 6 h. TM (6 µg ml^{-1}) was then added on each plate to induce ER stress overnight before imaging the next day.

Phenotypical assays to evaluate stress treatment

Percent crawling with osmotic stress was scored by counting the number of motile animals. An animal was considered non-motile if it did not show forward or backward motion for 5 s. Percent alive with paraquat stress was scored by counting the number of worms alive at the indicated hour. An animal was considered alive if it showed head motion and pharyngeal pumping for 5 s. Percent developed to L4 or young adult with TM treatment was scored by spotting L1 synchronous animals to indicated plates and counting animals reaching the fourth larval stage or young adult after 2.5 d following treatment with TM. The s.d. and mean values are shown throughout.

Growth rate assay

Five gravid young adults were allowed to lay eggs on each plate synchronously with or without stressors and removed after 3 h. Animals were staged at 62–68 h when more than 80% control animals with no stress treatment reached young adulthood. Before testing, animals were maintained under stress-free conditions at 20 °C for multiple generations, including no starvation and no obvious contamination.

RNAi screen

RNAi screening was performed on RNAi NGM agar plates. Animals were placed on RNAi plates and allowed to grow for 6 h. Plates were then treated with 400 µl diluted DMSO or TM (6 µg ml^{-1}) and allowed to soak in for 30 min. The induction of HSP-4p::GFP was imaged 22 h later.

Generation of CRISPR-Cas9 mutations

Dual HA-AID-tagged FASN-1 (HA::AID::GSGTGS::FASN-1::GSGTGS::AID::HA), caspase cleavage-resistant FASN-1 (D1593E) point mutation and CED-3::HA were generated using short-range HDR with *dpy-10* co-CRISPR method in the endogenous genomic locus. An extra single-copy transgene of FASN-NTF (HA::AID::GSGTGS::FASN-1 (aa2-aa1593)), FASN-NTF$^{\Delta linker}$ (HA::AID::GSGTGS::FASN-1(aa2-aa1138)), FASN-1-CTF (FASN-1 (aa1594 to aa2613)::GSGTGS::AID::HA) and FASN-1-CTF^{4-KO} was inserted into Mos1 transposon site LGIII Mos1_oxTi444 or LGI Mos1_ttTi4348 using the SEC CRISPR-Cas9 method.

For cell autonomy testing, a body-wall muscle promoter (myo-3) and intestine promoter (ges-1) were used to drive the expression of FASN-CTF as extra single-copy transgenes. To generate these tissue-specific-expressing FASN-CTF strains, CRISPR mutagenesis was used to insert one extra copy of each transgene in the LGIII Mos1_oxTi444 transposon site and crossing each of them into a ced-3 null mutant expressing the HSP-4p::GFP reporter, respectively. Strain's names, rescue templates and single-guide RNAs are shown in Supplementary Tables 1–3.

Imaging

For imaging analysis, animals were immobilized with 5% sodium azide (UN3287 ICCA) at the indicated time point. For HSP-4p::GFP, NLP-29p::GFP and GCS-1p::GFP stress reporter inductions, images were acquired using an Axiozoom microscope (Zeiss). For DHS-3::GFP LD visualization, images were acquired using a Nomarski microscope (Zeiss running Zen v.2.5) with ApoTome. All fluorescence quantifications were processed using Fiji (ImageJ v.1.54f). For quantification, the animal boundary was defined using bright-field imaging and the mean pixel intensity was calculated using a fluorescent image taken with the same field of view. Quantification was presented as FC to WT animals at 0 h for a given treatment. For confocal microscopy of Grx1-GFP2 strains, images were acquired using a Zeiss LSM900 equipped with Airyscan 2, GaAsP PMT detectors and 405/488/561/640-nm lasers running Zen v.3.4. Specifically, excitation by a 405-nm laser and a 488-nm laser was performed in tandem to determine the relative fractions of oxidized and reduced Grx1-roGFP2, respectively. Emissions were detected by a GaAsP PMT with no filters.

In vitro cleavage assay

Caspase cleavage reactions were performed as previously reported[55]. Purified human caspase-2 (R&D Systems 702-C2-010/CF), caspase-3 (R&D Systems 707-C3-010/CF) and caspase-8 (R&D Systems

705-C8-010/CF) were incubated with ^{35}S-labelled FASN fragments at 30 °C temperature overnight. ^{35}S-labelled substrates were synthesized fresh before cleavage reactions using a TNT system (Promega). Cleavage reactions were stopped by adding sample buffer and heating to 85 °C. Samples were resolved by SDS–PAGE on 4–16% gradient gels and dried before imaging.

Western blot
Animals were washed off plates using M9 and snap frozen with liquid nitrogen. Pellets were sonicated in lysis buffer containing 10 mM Tris, pH 7.4, 1 mM EDTA, 150 mM NaCl, 0.5% NP-40, Halt Protease and Phosphatase Inhibitor Cocktails (Fisher Scientific, PI78440) on ice. Approximately 5 µg of total protein was loaded per well and resolved on 4–20% gradient acrylamide gels. Anti-HA antibody from rabbit (Cell Signaling Technology, 3724S) was used at 1:1,000 dilution. Anti-actin (Bio-Rad, 12004163) antibody was used at 1:4,000 dilution for loading control.

Immunoprecipitation of caspase
An HA tag was inserted at the C terminus of CED-3 using CRISPR mutagenesis. Because CED-3 expression is extremely low, HA immunoprecipitation (IP) was undertaken to observe the expression and processing of CED-3. Synchronized L4 was treated with 4 µg ml^{-1} TM for 18 h and 100 µl worm pellet was collected and snap frozen in liquid N$_2$ for IP. The worm pellet was lysed using sonication and the protein concentration was determined using a BCA assay. IP was performed using HA tag (C29F4) rabbit monoclonal antibody (Cell Signaling Technology, 11846S) at 1:200 dilution for 4 h at 4 °C. Western blot was performed using mouse monoclonal antibody (Cell Signaling Technology, 2367S). Actin (Bio-Rad, 12004163) was used as a loading control of the input.

Free fatty acid isotopologues
Synchronized L4 animals were collected and incubated with PBS in 50% deuterium-labelled water for 20 h with rotation. UV-killed bacteria were used as a food source to limit additional metabolism. Animals were collected in M9 and the worm pellet was snap frozen in liquid N$_2$. Worms were lysed in 1 ml ice-cold 50% methanol with sonication and 1% BHT was added to prevent lipid oxidation. Free fatty acids were extracted by mixing 0.5 ml chloroform to each sample to reach a methanol:water:chloroform ratio of 1:1:1 ($v/v/v$). Samples were then spun at 1,000g for 5 min and the organic phases (lower) were collected and dried under air flow. Then, 100 µl 1 N HCl and 200 µl toluene were sequentially added with vortexing to each sample. After a brief spin, the toluene solution (top layer) was decanted into a fresh Eppendorf tube and evaporated to dryness. Then, 100 µl of TBDMS solution (Sigma) was added to each sample with vortexing and heated to 70 °C for 1 h for fatty acid derivatization. Samples were then transferred to gas chromatograph vials and run on an Agilent 6970 gas chromatograph networked to an Agilent 5973 Mass Selective Detector. Fragment ion m/z 313–329 was used to monitor enrichment in palmitate.

Metabolomics
Synchronized very young adults before egg laying were collected using M9 and washed 2× with Milli-Q water. The worm pellet was about 100 mg wet weight. Then, 85% methanol (400 µl) was added with 0.1 mm zirconia beads (RPI 9833) for each extraction using a FastPrep-24 sample preparation system (MP Biomedicals). The supernatant was transferred to a clean tube after 1 min of 16,000g centrifugation. A BCA assay was used to determine the protein concentration. Samples were dried with a speed vacuum (Eppendorf) and resuspended in acetonitrile/water for metabolomics analysis.

Untargeted metabolomics was performed by Creative Proteomics. A targeted metabolomics screen was conducted by the University of Texas Southwestern (UTSW) CRI metabolomics core. A t-test was used to evaluate the significance in metabolite change between two sets of samples. The MetaboAnalyst (www.metaboanalyst.ca) pathway

enrichment module was used for pathway analysis using the SMPDB. The ranking of the enrichment pathway was based on both P value and the percent of metabolites in a given pathway represented in the metabolomics panel. GraphPad was used for PCA and eigenvalue calculations.

Seahorse measurement of oxygen consumption rate
Plates of synchronized adult worms were collected by washing with 1 ml M9 buffer. The worms were allowed to settle to the bottom by gravity and then rinsed three times with fresh M9 buffer to remove bacteria. The worms were then plated on sterile NGM plates in a 300-µl drop of M9 buffer. The worms were allowed to crawl out of the drop and then placed in a seahorse assay plate in 200 µl M9 buffer. Each well contained 40 adult worms. The worms were allowed to acclimate to the buffer for 30 min and then OCR was measured three times using a seahorse XFp. The amount of mitochondrial-specific respiration was determined by injecting sodium azide (40 mM final concentration) and measuring the residual OCR. Each data point represents the average of three OCR measurements. Each experiment contained three independent biological replicates.

mRNA-seq
Synchronous young-adult-stage animals were collected in TRIzol reagent (Invitrogen, 15596-026). Total RNA was extracted and DNase treated. Three independent biological replicates of each treatment and genotype were collected. Libraries were generated, sequenced and analysed for differential gene expression by the UTSW McDermott Center Next-Generation Sequencing Core. For messenger RNA-seq, single-end 76-bp-read-length fastq files were checked for quality using fastqc (v.0.11.2) and fastq_screen (v.0.4.4). Reads were quality trimmed using fastq-mcf (ea-utils, v.1.1.2-806). Trimmed fastq files were mapped to the *C. elegans* genome using STAR (v.2.5.3a). Duplicate alignments were removed using Picard Tools (v.2.10). Read counts were generated using featureCounts (subread) for coding genes from iGenomes (RefSeq). Normalized read counts were generated using edgeR. WormBase gene set enrichment analysis tools were used for Gene Ontology analyses.

DCP-Bio1 labelling and proteomic analysis
Primary cOBs were isolated as described previously[56]. cOBs were cultured with or without 250 µM H$_2$O$_2$ for 24 h before DCP-Bio1 labelling. DCP-Bio1 selectively reacts with cysteine sulfenic acid thus detecting oxidation products. Cells were scraped, lysed and reacted with the cysteine sulfenic acid probe, 3-(2,4-dioxocyclohexyl) propyl appended to biotin (DCP-Bio1) for 1.5 h in a modified lysis buffer containing 50 mM Tris-HCl (pH 7.5), 100 mM NaCl, 0.1% SDS, 0.5% sodium deoxycholate, 0.5% NP-40, 0.5% Triton X-100, 50 mM NaF, 1 mM phenylmethylsulfonyl fluoride, 1 mM DCP-Bio1, 100 µM diethylenetriamine pentaacetic acid, 10 mM N-ethylmaleimide, 10 mM iodoacetamide, 200 U ml^{-1} catalase and protease inhibitor cocktail. After centrifugation at 9,600g for 10 min, unreacted DCP-Bio1 in the supernatant was removed using Bio-Rad P6-Spin columns. DCP-Bio1-labelled proteins were immunoprecipitated using a Pierce Classic Magnetic IP kit and purified with 10% SDS–PAGE gel. Proteomic analysis of gel slices was performed by the University of Texas Southwestern Proteomics Core.

Mouse fasting assay
Mice used in this study were all WT males on C57BL/6J background. Mice were housed in a specific pathogen-free facility with a 12-h light–dark cycle and fed with standard rodent chow ad libitum. The housing temperature range was 68–79 °F and humidity was 30–70%. During fasting, each mouse was individually caged with free access to water. Body weight was monitored every 24 h. Mice were killed at the end of 36 h of fasting. The liver was collected and snap frozen in liquid nitrogen. All animal use was approved by the Institutional Animal Care and Use Committee at the UTSW Medical Center.

Statistics

Statistical analyses and *P* values are provided in figures, legends, Supplementary Data 1–3 and Source Data.

Reporting summary

Further information on research design is available in the Nature Portfolio Reporting Summary linked to this article.

Data availability

The mRNA-seq data generated in this study have been deposited in the Gene Expression Omnibus database under accession code GSE226048. The remaining data generated in this study are provided in the Source Data file. Source data are provided with this paper.

References

1. Joshi, A. K., Rangan, V. S., Witkowski, A. & Smith, S. Engineering of an active animal fatty acid synthase dimer with only one competent subunit. *Chem. Biol.* **10**, 169–173 (2003).
2. Wakil, S. J., Stoops, J. K. & Joshi, V. C. Fatty acid synthesis and its regulation. *Annu. Rev. Biochem.* **52**, 537–579 (1983).
3. Rohrig, F. & Schulze, A. The multifaceted roles of fatty acid synthesis in cancer. *Nat. Rev. Cancer* **16**, 732–749 (2016).
4. Judy, M. E. et al. A shift to organismal stress resistance in programmed cell death mutants. *PLoS Genet.* **9**, e1003714 (2013).
5. Weaver, B. P. et al. Non-canonical caspase activity antagonizes p38 MAPK stress-priming function to support development. *Dev. Cell* **53**, 358–369 (2020).
6. Putinski, C., Abdul-Ghani, M., Brunette, S., Burgon, P. G. & Megeney, L. A. Caspase cleavage of gelsolin is an inductive cue for pathologic cardiac hypertrophy. *J. Am. Heart Assoc.* **7**, e010404 (2018).
7. Wilson, C. H. et al. Age-related proteostasis and metabolic alterations in caspase-2-deficient mice. *Cell Death Dis.* **6**, e1615 (2015).
8. Pinan-Lucarre, B. et al. The core apoptotic executioner proteins CED-3 and CED-4 promote initiation of neuronal regeneration in *Caenorhabditis elegans*. *PLoS Biol.* **10**, e1001331 (2012).
9. Brunette, S., Sharma, A., Bell, R., Puente, L. & Megeney, L. A. Caspase 3 exhibits a yeast metacaspase proteostasis function that protects mitochondria from toxic TDP43 aggregates. *Micro. Cell* **10**, 157–169 (2023).
10. Yuan, W. et al. Modulating p38 MAPK signaling by proteostasis mechanisms supports tissue integrity during growth and aging. *Nat. Commun.* **14**, 4543 (2023).
11. Kim, J. Y. et al. ER stress drives lipogenesis and steatohepatitis via caspase-2 activation of S1P. *Cell* **175**, 133–145 (2018).
12. Gutscher, M. et al. Real-time imaging of the intracellular glutathione redox potential. *Nat. Methods* **5**, 553–559 (2008).
13. Back, P. et al. Exploring real-time in vivo redox biology of developing and aging *Caenorhabditis elegans*. *Free Radic. Biol. Med.* **52**, 850–859 (2012).
14. Li, J., Billiar, T. R., Talanian, R. V. & Kim, Y. M. Nitric oxide reversibly inhibits seven members of the caspase family via S-nitrosylation. *Biochem. Biophys. Res. Commun.* **240**, 419–424 (1997).
15. Dimmeler, S., Haendeler, J., Nehls, M. & Zeiher, A. M. Suppression of apoptosis by nitric oxide via inhibition of interleukin-1β-converting enzyme (ICE)-like and cysteine protease protein (CPP)-32-like proteases. *J. Exp. Med.* **185**, 601–607 (1997).
16. Hampton, M. B. & Orrenius, S. Dual regulation of caspase activity by hydrogen peroxide: implications for apoptosis. *FEBS Lett.* **414**, 552–556 (1997).
17. Cao, S. S. & Kaufman, R. J. Endoplasmic reticulum stress and oxidative stress in cell fate decision and human disease. *Antioxid. Redox Signal.* **21**, 396–413 (2014).
18. Kritsiligkou, P. et al. Endoplasmic reticulum (ER) stress-induced reactive oxygen species (ROS) are detrimental for the fitness of a thioredoxin reductase mutant. *J. Biol. Chem.* **293**, 11984–11995 (2018).
19. Jayakumar, A. et al. Human fatty acid synthase: properties and molecular cloning. *Proc. Natl Acad. Sci. USA* **92**, 8695–8699 (1995).
20. Semenkovich, C. F., Coleman, T. & Fiedorek, F. T. Jr. Human fatty acid synthase mRNA: tissue distribution, genetic mapping, and kinetics of decay after glucose deprivation. *J. Lipid Res.* **36**, 1507–1521 (1995).
21. Sokolovic, M. et al. The transcriptomic signature of fasting murine liver. *BMC Genom.* **9**, 528 (2008).
22. Wasselin, T. et al. Exacerbated oxidative stress in the fasting liver according to fuel partitioning. *Proteomics* **14**, 1905–1921 (2014).
23. Lee, K. Z., Kniazeva, M., Han, M., Pujol, N. & Ewbank, J. J. The fatty acid synthase fasn-1 acts upstream of WNK and Ste20/GCK-VI kinases to modulate antimicrobial peptide expression in *C. elegans* epidermis. *Virulence* **1**, 113–122 (2010).
24. Holdorf, A. D. et al. WormCat: an online tool for annotation and visualization of *Caenorhabditis elegans* genome-scale data. *Genetics* **214**, 279–294 (2020).
25. Bailey, A. P. et al. Antioxidant role for lipid droplets in a stem cell niche of *Drosophila*. *Cell* **163**, 340–353 (2015).
26. Henne, W. M., Reese, M. L. & Goodman, J. M. The assembly of lipid droplets and their roles in challenged cells. *EMBO J.* **37**, e98947 (2018).
27. Herms, A. et al. Cell-to-cell heterogeneity in lipid droplets suggests a mechanism to reduce lipotoxicity. *Curr. Biol.* **23**, 1489–1496 (2013).
28. Zhang, P. et al. Proteomic study and marker protein identification of *Caenorhabditis elegans* lipid droplets. *Mol. Cell Proteom.* **11**, 317–328 (2012).
29. Diot, C. et al. Bacterial diet modulates tamoxifen-induced death via host fatty acid metabolism. *Nat. Commun.* **13**, 5595 (2022).
30. Perez, M. A., Magtanong, L., Dixon, S. J. & Watts, J. L. Dietary lipids induce ferroptosis in *Caenorhabditis elegans* and human cancer cells. *Dev. Cell* **54**, 447–454 (2020).
31. Princova, J. et al. Perturbed fatty-acid metabolism is linked to localized chromatin hyperacetylation, increased stress-response gene expression and resistance to oxidative stress. *PLoS Genet.* **19**, e1010582 (2023).
32. Kim, H. E. et al. Lipid biosynthesis coordinates a mitochondrial-to-cytosolic stress response. *Cell* **166**, 1539–1552 (2016).
33. Wei, X. et al. Fatty acid synthesis configures the plasma membrane for inflammation in diabetes. *Nature* **539**, 294–298 (2016).
34. Avraham, O. et al. Satellite glial cells promote regenerative growth in sensory neurons. *Nat. Commun.* **11**, 4891 (2020).
35. Schroeder, L. K. et al. Function of the *Caenorhabditis elegans* ABC transporter PGP-2 in the biogenesis of a lysosome-related fat storage organelle. *Mol. Biol. Cell* **18**, 995–1008 (2007).
36. Brooks, K. K., Liang, B. & Watts, J. L. The influence of bacterial diet on fat storage in *C. elegans*. *PLoS ONE* **4**, e7545 (2009).
37. O'Rourke, E. J., Soukas, A. A., Carr, C. E. & Ruvkun, G. *C. elegans* major fats are stored in vesicles distinct from lysosome-related organelles. *Cell Metab.* **10**, 430–435 (2009).
38. Zhang, S. O., Trimble, R., Guo, F. & Mak, H. Y. Lipid droplets as ubiquitous fat storage organelles in *C. elegans*. *BMC Cell Biol.* **11**, 96 (2010).
39. Dowen, R. H., Breen, P. C., Tullius, T., Conery, A. L. & Ruvkun, G. A microRNA program in the *C. elegans* hypodermis couples to intestinal mTORC2/PQM-1 signaling to modulate fat transport. *Genes Dev.* **30**, 1515–1528 (2016).
40. Gao, Q. et al. Pet10p is a yeast perilipin that stabilizes lipid droplets and promotes their assembly. *J. Cell Biol.* **216**, 3199–3217 (2017).

41. Mosquera, J. V., Bacher, M. C. & Priess, J. R. Nuclear lipid droplets and nuclear damage in *Caenorhabditis elegans*. *PLoS Genet.* **17**, e1009602 (2021).

42. Steinbaugh, M. J. et al. Lipid-mediated regulation of SKN-1/Nrf in response to germ cell absence. *eLife* **4**, e07836 (2015).

43. Glover-Cutter, K. M., Lin, S. & Blackwell, T. K. Integration of the unfolded protein and oxidative stress responses through SKN-1/Nrf. *PLoS Genet.* **9**, e1003701 (2013).

44. Hourihan, J. M., Moronetti Mazzeo, L. E., Fernandez-Cardenas, L. P. & Blackwell, T. K. Cysteine sulfenylation directs IRE-1 to activate the SKN-1/Nrf2 antioxidant response. *Mol. Cell* **63**, 553–566 (2016).

45. Han, J. & Kaufman, R. J. The role of ER stress in lipid metabolism and lipotoxicity. *J. Lipid Res.* **57**, 1329–1338 (2016).

46. Schieber, M. & Chandel, N. S. ROS function in redox signaling and oxidative stress. *Curr. Biol.* **24**, R453–R462 (2014).

47. D'Autreaux, B. & Toledano, M. B. ROS as signalling molecules: mechanisms that generate specificity in ROS homeostasis. *Nat. Rev. Mol. Cell Biol.* **8**, 813–824 (2007).

48. Chouchani, E. T., James, A. M., Fearnley, I. M., Lilley, K. S. & Murphy, M. P. Proteomic approaches to the characterization of protein thiol modification. *Curr. Opin. Chem. Biol.* **15**, 120–128 (2011).

49. Meng, J. et al. Global profiling of distinct cysteine redox forms reveals wide-ranging redox regulation in *C. elegans*. *Nat. Commun.* **12**, 1415 (2021).

50. Murray, C. I. & Van Eyk, J. E. Chasing cysteine oxidative modifications: proteomic tools for characterizing cysteine redox status. *Circ. Cardiovasc. Genet.* **5**, 591 (2012).

51. Reddie, K. G. & Carroll, K. S. Expanding the functional diversity of proteins through cysteine oxidation. *Curr. Opin. Chem. Biol.* **12**, 746–754 (2008).

52. Paek, J. et al. Mitochondrial SKN-1/Nrf mediates a conserved starvation response. *Cell Metab.* **16**, 526–537 (2012).

53. Ewald, C. Y. et al. NADPH oxidase-mediated redox signaling promotes oxidative stress resistance and longevity through memo-1 in *C. elegans*. *eLife* **6**, e19493 (2017).

54. Statzer, C. et al. ATF-4 and hydrogen sulfide signalling mediate longevity in response to inhibition of translation or mTORC1. *Nat. Commun.* **13**, 967 (2022).

55. Weaver, B. P., Weaver, Y. M., Mitani, S. & Han, M. Coupled caspase and N-end rule ligase activities allow recognition and degradation of pluripotency factor LIN-28 during non-apoptotic development. *Dev. Cell* **41**, 665–673 (2017).

56. Shen, L. et al. SLC38A2 provides proline to fulfill unique synthetic demands arising during osteoblast differentiation and bone formation. *eLife* **11**, e76963 (2022).

Acknowledgements

Author contributions

Conceptualization was the responsibility of H.W., Y.M.W. and B.P.W. Methodology and investigation were the responsibility of H.W., Y.M.W., C.Y., Y.Z., G.H., M.S., C.M.K. and B.P.W. Formal analysis was conducted by H.W., Y.M.W., C.Y., Y.Z., G.H., M.S., C.M.K., R.J.D. and B.P.W. Writing was carried out by H.W., Y.M.W., R.J.D. and B.P.W. Supervision of the study was carried out by Y.M.W., R.J.D. and B.P.W. Funding acquisition was the responsibility of R.J.D., C.M.K., M.S. and B.P.W.

Competing interests

Additional information

Extended data is available for this paper at https://doi.org/10.1038/s42255-023-00939-z.

Supplementary information The online version contains supplementary material available at https://doi.org/10.1038/s42255-023-00939-z.

Correspondence and requests for materials should be addressed to Benjamin P. Weaver.
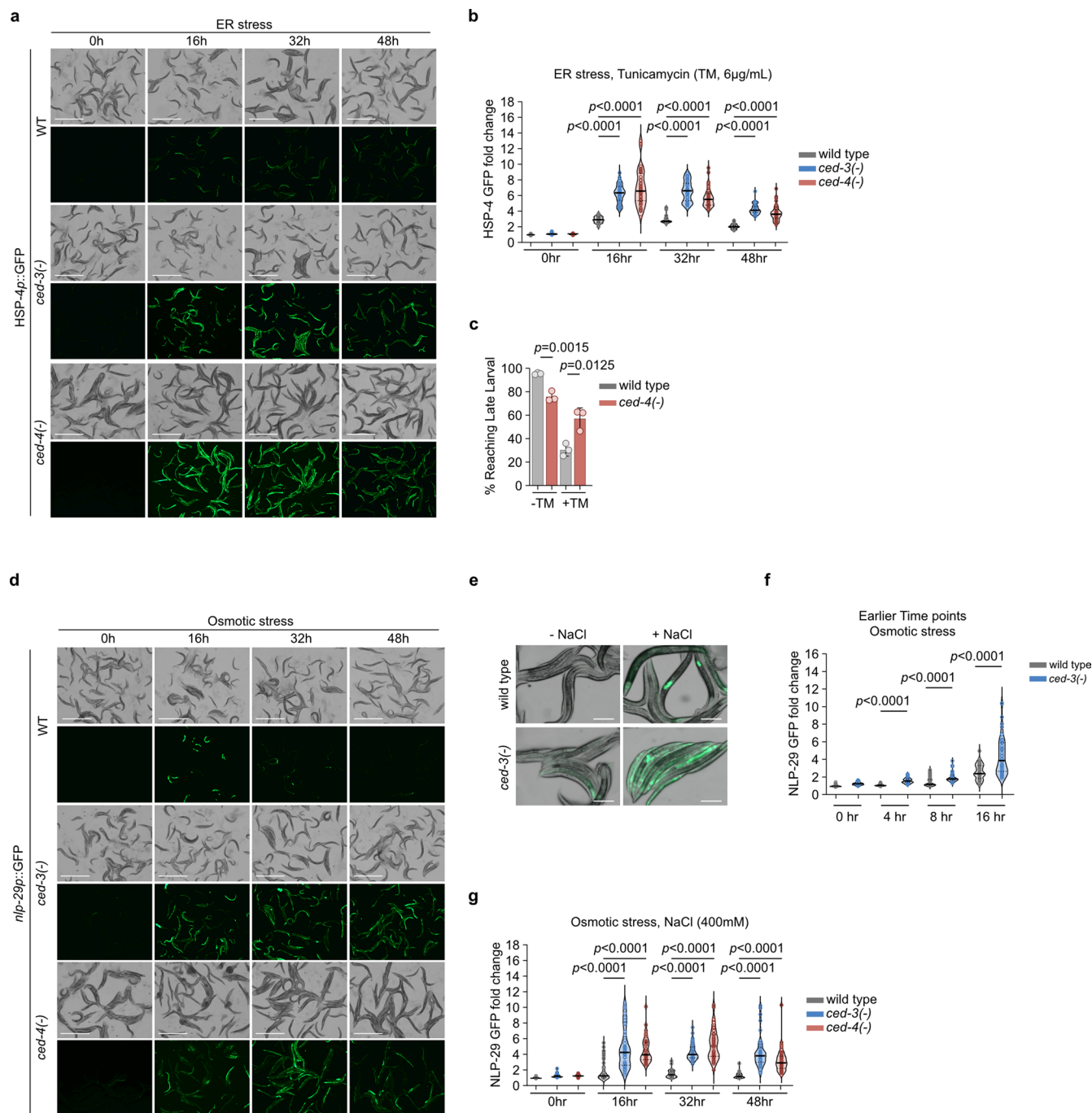
Peer review information *Nature Metabolism* thanks Andrew Dillin, Maria Ermolaeva and the other, anonymous, reviewer(s) for their contribution to the peer review of this work. Primary Handling Editor: Alfredo Giménez-Cassina, in collaboration with the *Nature Metabolism* team.

Reprints and permissions information is available at www.nature.com/reprints.

Publisher's note Springer Nature remains neutral with regard to jurisdictional claims in published maps and institutional affiliations.
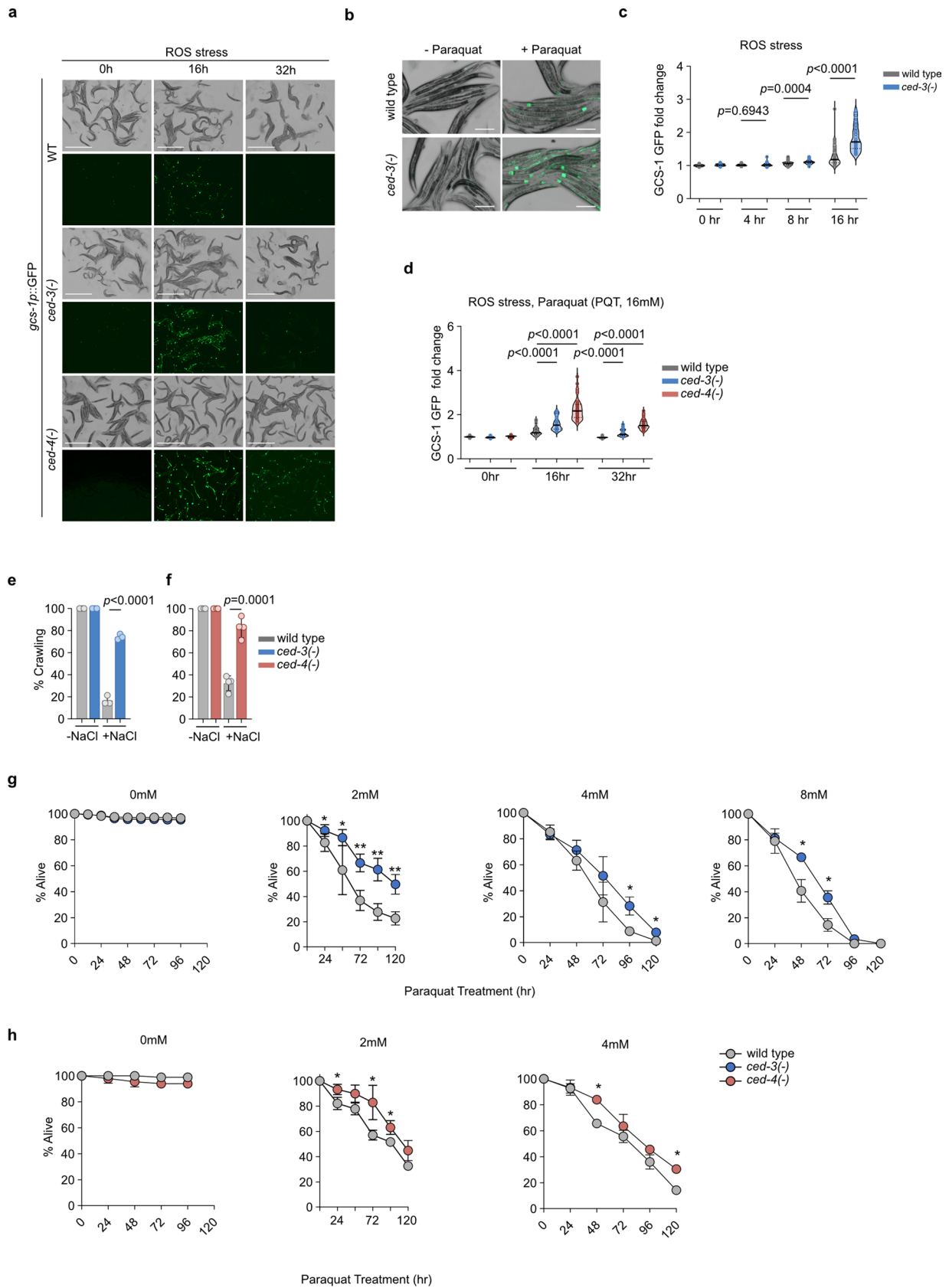
Extended Data Fig. 1 | Elevated ER and osmotic stress responses in *ced-3(-)* and *ced-4(-)* animals. a-b, representative images (**a**) and quantification (**b**) of HSP-4p::GFP stress reporter induction under ER stress at different time points. Wild type and *ced-3(-)* were repeated from main figure for comparison to *ced-4(-)* animals. n = 40 animals. **c**, quantification of *ced-4(-)* animals escaping larval arrest with tunicamycin (TM) treatment to induce ER stress. n = 3 biological replicates. mean ± SD. **d**, representative images of NLP-29p::GFP (antimicrobial peptide) stress reporter induction with 400 mM NaCl treatment to induce osmotic stress in *ced-3(-)* and *ced-4(-)* animals at different time points. **e**, digital zoom in of 0 h and 32 h images shown in **d** of epidermal NLP-29p::GFP reporter induction in

ced-3(-) animals under osmotic stress. **f**, quantification of NLP-29p::GFP stress reporter expression under osmotic stress at early time points. n = 50 animals. **g**, quantification of NLP-29p::GFP stress reporter expression for both *ced-3(-)* and *ced-4(-)* animals. n = 40 animals. For **a,d**, scale bar, 1 mm. For **e**, scale bar, 200μm. For **b,f,g** each circle represents one animal. Mean pixel intensity of each animal was normalized to mean value of wild type at 0 hr (no stress) and plotted as fold change. Violin plots show median (solid line) with quartiles (dashed line). *p* values were calculated using Mann-Whitney, two-tailed test (**b,f,g**) and unpaired two-tailed t-test (**c**).

Extended Data Fig. 2 | See next page for caption.

Extended Data Fig. 2 | Elevated ROS stress response in *ced-3(-)* and *ced-4(-)* animals. a, representative images of GCS-1p::GFP (glutamate-cysteine ligase) stress reporter induction with 16 mM paraquat (PQT) treatment to induce ROS stress in *ced-3(-)* and *ced-4(-)* animals at different time points. scale bar, 1 mm. **b**, digital zoom in of 0 h and 16 h of neuronal and intestinal GCS-1p::GFP reporter induction in *ced-3(-)* animals under ROS stress. scale bar, 200μm. **c**, quantification of GCS-1p::GFP stress reporter induction under ROS stress at early time points. n = 50 animals. **d**, quantification of GCS-1p::GFP stress reporter induction for both *ced-3(-)* and *ced-4(-)* animals. n = 40 animals. **e-f**, quantification of motile animals for *ced-3(-)* (**e**) and *ced-4(-)* (**f**) mutants with sodium chloride (NaCl) treatment to induce osmotic stress. *ced-3(-)* n = 3 and *ced-4(-)* n = 4 biological

replicates. Mean ± SD. **g-h**, survival for *ced-3(-)* (**g**) and *ced-4(-)* (**h**) mutants with increasing concentration of PQT to induce ROS stress. n = 3 biological replicates. Mean ± SD, total animals examined in **g**, 0 mM, n = 532; 2 mM, n = 579, 4 mM, n = 493, 8 mM, n = 567; total animals examined in **h**, 0 mM, n = 505; 2 mM, n = 567, 4 mM, n = 286. *, $p < 0.05$; **, $p < 0.0001$. Exact p value see Source Data. For **c,d**, each circle represents one animal. Mean pixel intensity of each animal was normalized to mean value of wild type at 0 hr (no stress) and plotted as fold change. Violin plots show median (solid line) with quartiles (dashed line). p values were calculated using Mann-Whitney, two-tailed test (**c,d**) and unpaired two-tailed t-test (**e,f,g,h**).
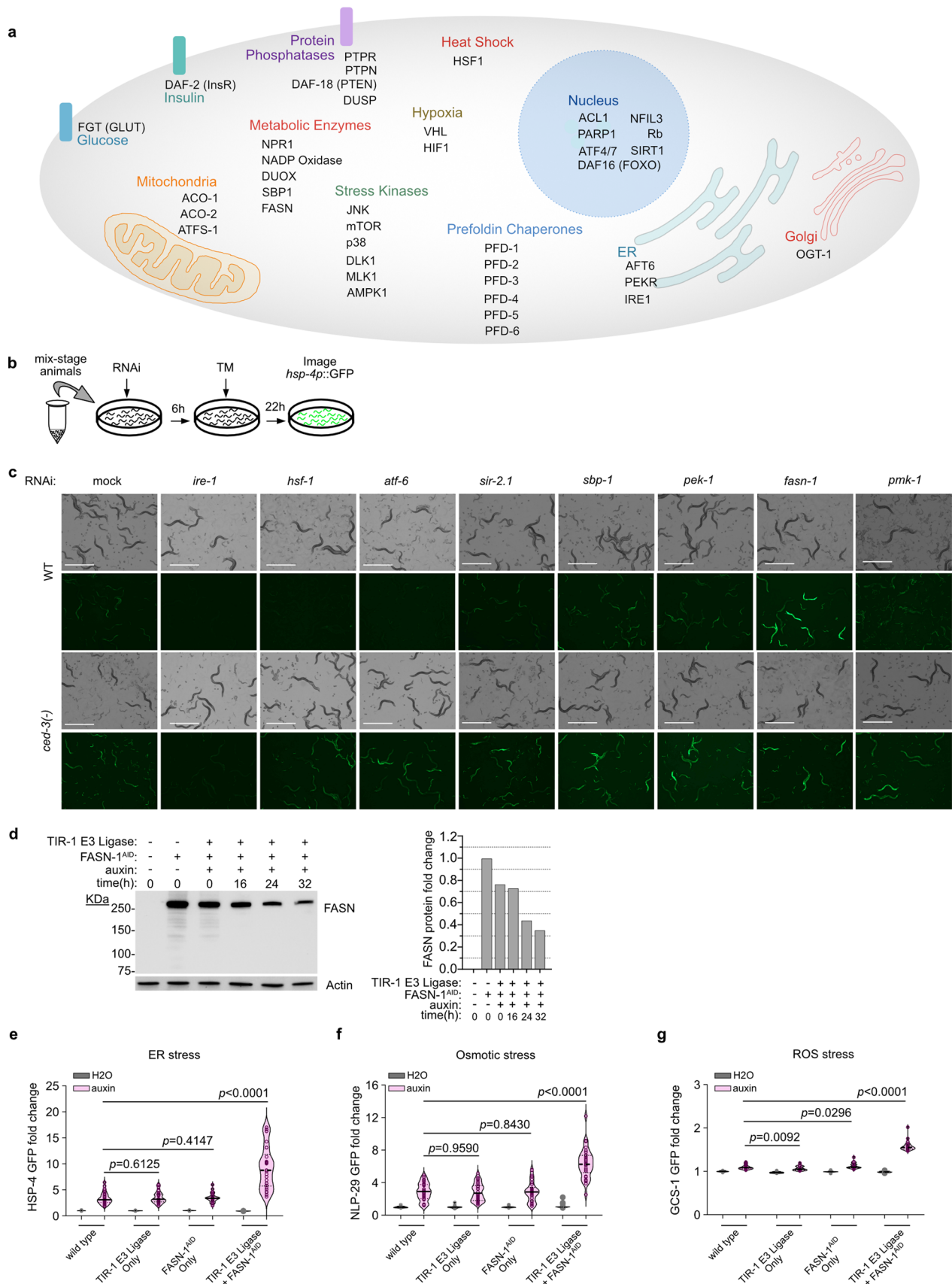
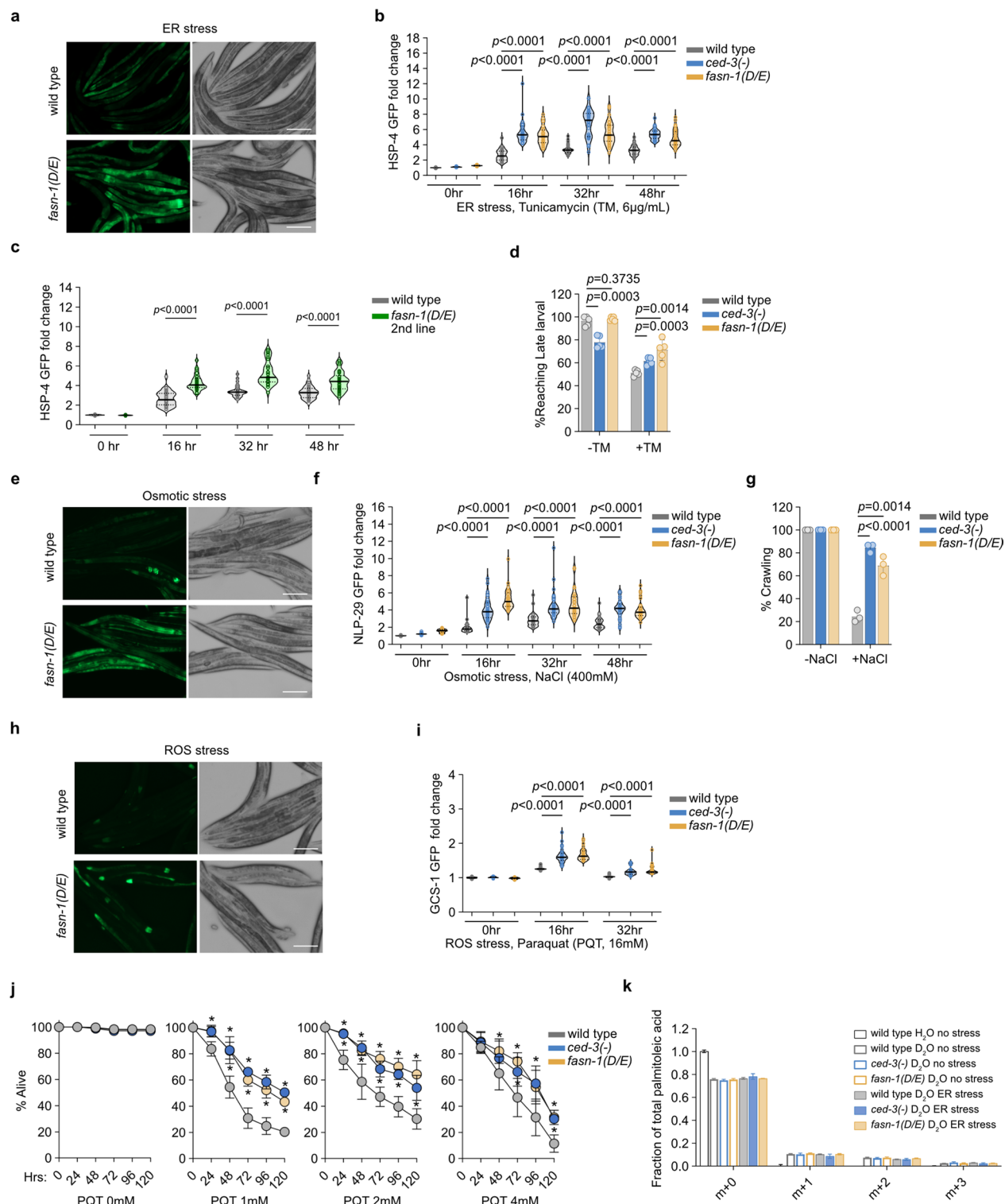Extended Data Fig. 3 | See next page for caption.

Extended Data Fig. 3 | Target RNAi screen to reveal factors modulating heightened stress responses and characterization of auxin-induced degradation of FASN-1. a, diagram showing all factors in multiple stress response pathways included in the targeted RNAi screen. **b**, work flow of RNAi screen. **c**, representative images of raw images from RNAi screen. Scale bar, 1 mm. Screen was performed once with duplicates. Candidates were later confirmed with one additional round of confirmation screen. **d**, optimization for time-dependent auxin-induced degradation of FASN. Optimization was performed once to show timing of degradation. **e-g**, HSP-4p:: GFP (**e**), NLP-29p:: GFP (**f**) and GCS-1p:: GFP (**g**) signals are not affected by expressing TIR-1 E3 ligase transgene or insertion of auxin induced degron at the endogenous locus of *fasn-1*. Wild type auxin treated and TIR-1 E3 Ligase + FASN[AID] auxin treated conditions were repeats from main figures for comparison. n = 30 animals for each condition. *p* values were calculated using Mann-Whitney, two-tailed test.
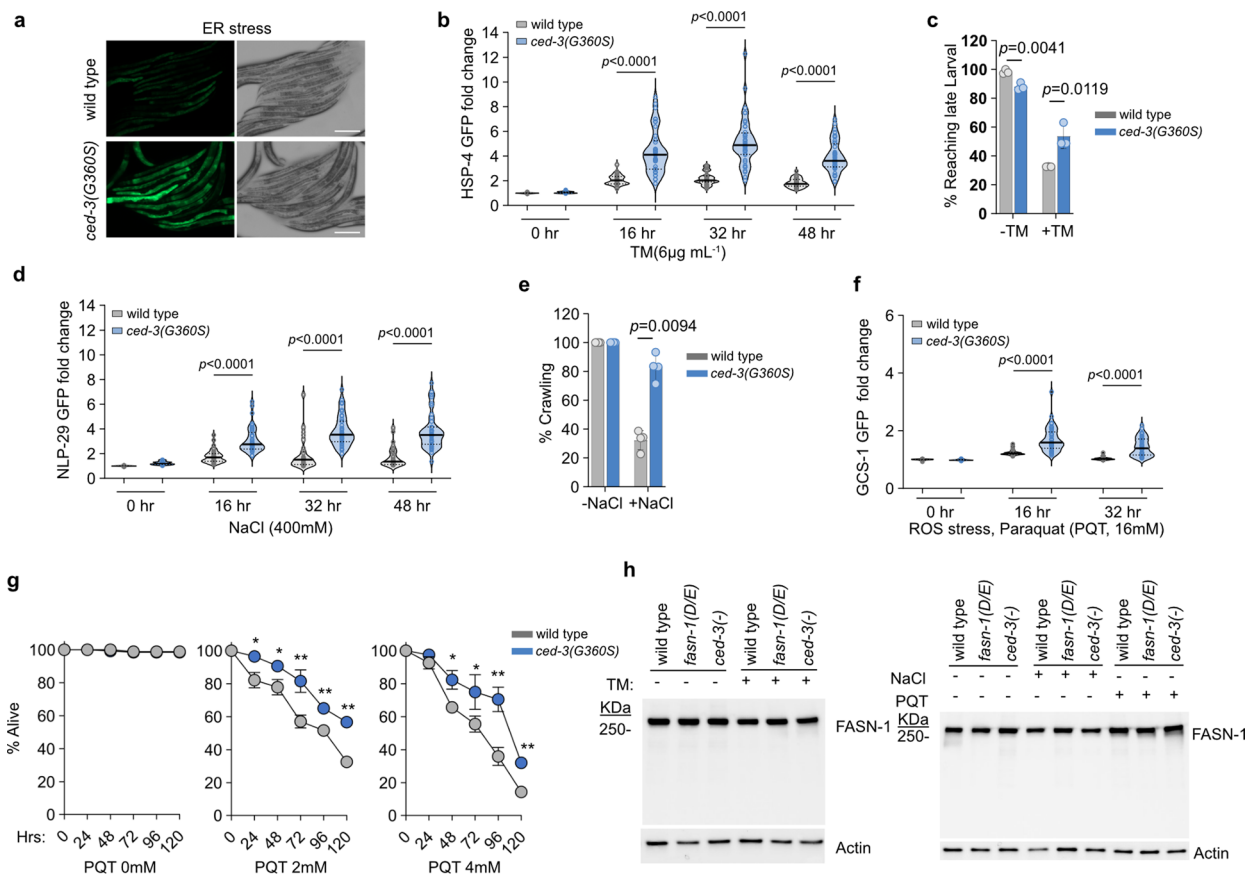
Extended Data Fig. 4 | Elevated ER, osmotic and ROS stress responses in *ced-3(G360S)* **active site mutant animals and** *in vivo* **expression of cleavage resistant** *fasn-1(D/E)* **protein. a**, representative images of HSP-4p::GFP stress reporter induction under ER stress in *ced-3(G360S)* animals. scale bar, 200µm. **b**, quantification of HSP-4::GFP stress reporter induction in *ced-3(G360S)* animals under ER stress at different time points. n = 40 animals. Treatment at 32 hr was repeated from main figure (Fig. 2a) for comparison. **c**, quantification of *ced-3(G360S)* animals escaping larval arrest with tunicamycin (TM) treatment to induce ER stress. n = 3 biological replicates. mean ± SD. **d**, quantification of NLP-29p::GFP stress reporter induction in *ced-3(G360S)* animals under osmotic stress at different time points. n = 40 animals. **e**, quantification of motility *ced-3(G360S)* mutants under osmotic stress. n = 4 biological replicates. mean ± SD. **f**, quantification of GCS-1p::GFP stress reporter induction in *ced-3(G360S)*
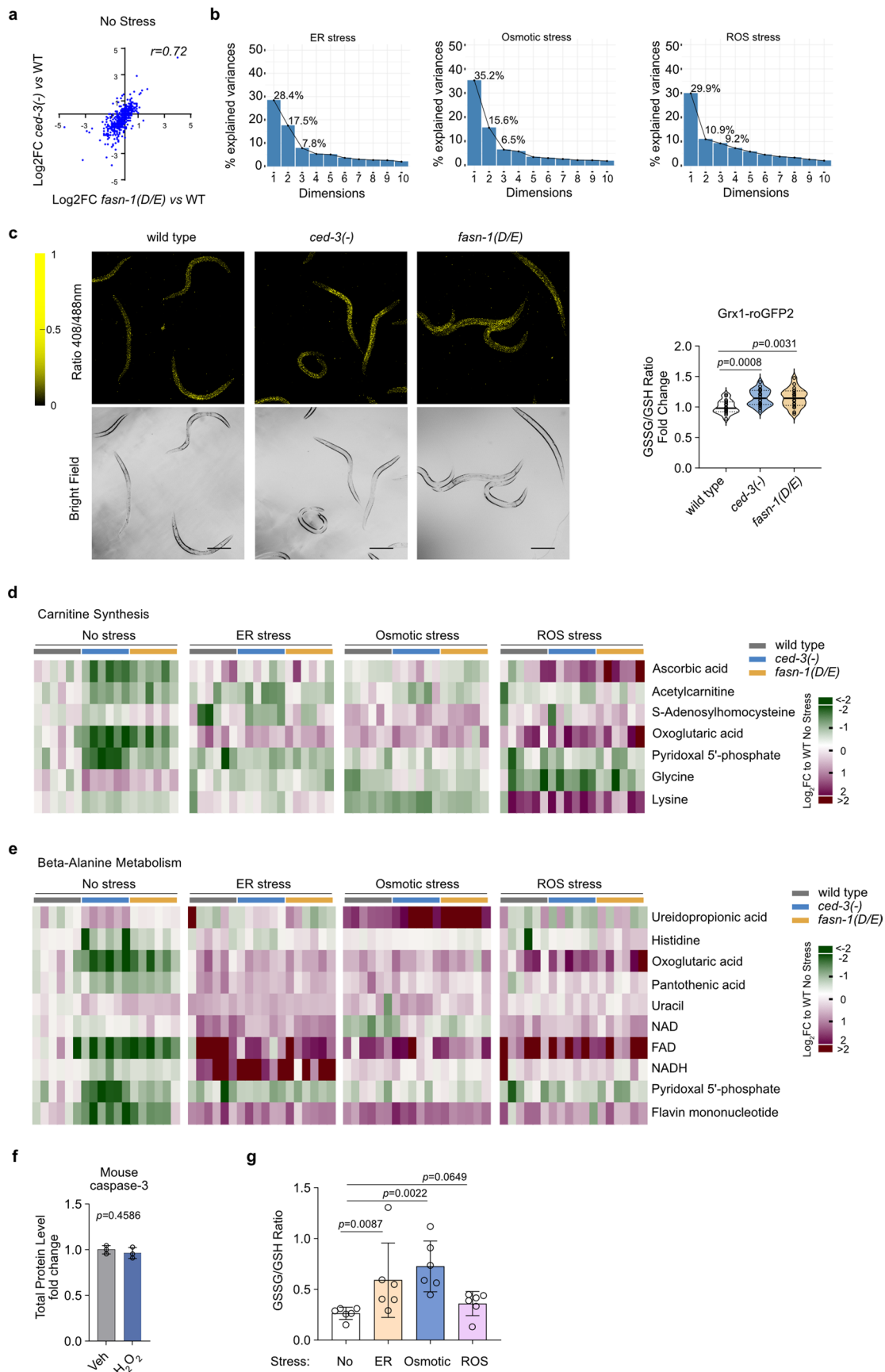
animals under ROS stress at different time points. n = 40 animals. **g**, survival for *ced-3(G360S)* animals with increasing concentration of PQT to induce ROS stress. n = 3 biological replicates. Mean ± SD, total animals examined, 0 mM, n = 218; 2 mM, n = 354, 4 mM, n = 286. *, $p < 0.05$. **, $p < 0.01$. Exact p value see Source Data. **h**, Western blot analyses of endogenous FASN-1 tagged with HA-AID tag in the absence of TIR-1 Ligase to allow expression under no stress, ER stress (TM), osmotic (NaCl) and ROS (PQT) stress in wild type, *ced-3(-)* and *fasn-1(D/E)* mutant animals. Western blot was performed once to shown no change in expression. For **b,d,f**, each circle represents one animal. Mean pixel intensity of each animal was normalized to mean value of wild type at 0 hr (no stress) and plotted as fold change. Violin plots show median (solid line) with quartiles (dashed line). p values were calculated using two-tailed Mann-Whitney test (**b,d,f**) and unpaired, two-tailed t-test (**c,e,g**).

Extended Data Fig. 5 | See next page for caption.

Extended Data Fig. 5 | Elevated ER, osmotic and ROS stress responses in cleavage-resistant *fasn-1(D/E)* mutant animals. a, representative images of HSP-4p::GFP stress reporter induction under ER stress in *fasn-1(D/E)* animals. scale bar, 200μm. **b**, quantification of HSP-4::GFP stress reporter induction in *fasn-1(D/E)* animals under ER stress at different time points. Treatment at 32 hr was repeated from main figure (Fig. 2f) for comparison. n = 30 animals. **c**, quantification of HSP-4::GFP stress reporter induction in a second CRISPR line of *fasn-1(D/E)* animals under ER stress at different time points. n = 30 animals. **d**, quantification of *fasn-1(D/E)* animals escaping larval arrest with tunicamycin (TM) treatment to induce ER stress. n = 5 biological replicates. mean ± SD. **e**, representative images of NLP-29p::GFP stress reporter induction under osmotic stress in *fasn-1(D/E)* animals. scale bar, 200μm. **f**, quantification of NLP-29p::GFP stress reporter induction in *fasn-1(D/E)* animals under osmotic stress at different time points. Treatment at 32 hr was repeated from main figure (Fig. 2f) for comparison. n = 30 animals. **g**, quantification of *fasn-1(D/E)* animals

motility with NaCl treatment to induce osmotic stress. n = 3 biological replicates. mean ± SD. **h**, representative images of GCS-1p::GFP stress reporter induction under ROS stress in *fasn-1(D/E)* animals. scale bar, 200μm. **i**, quantification of GCS-1p::GFP stress reporter induction in *fasn-1(D/E)* animals under ROS stress at different time points. Treatment at 16 hr was repeated from main figure (Fig. 2f) for comparison. n = 30 animals. **j**, survival for *fasn-1(D/E)* animals with increasing concentration of PQT to induce ROS stress. n = 5 biological replicates. Mean ± SD, total animals examined, 0 mM, n = 593; 1 mM, n = 604; 2 mM, n = 621; 4 mM, n = 536. *, $p < 0.05$. Exact p value see Source Data. **k**, measurement of palmitoleic acid synthesis using 50% deuterated water (D_2O) labeling for 16 hours in the presence or absence of ER stress. m + 0, unlabeled palmitoleic acid. m + 1, m + 2, m + 3 are deuterium-labeled representing newly synthesized palmitoleic acid. n = 3 biological samples. Mean ± SD. p values were calculated using Mann-Whitney test (**b,f,i**) and unpaired t-test (**d,g,j**).

a No Stress

Log2FC *ced-3(-) vs* WT vs Log2FC *fasn-1(D/E) vs* WT, *r=0.72*

b ER stress: 28.4%, 17.5%, 7.8% % explained variances across Dimensions 1–10. Osmotic stress: 35.2%, 15.6%, 6.5%. ROS stress: 29.9%, 10.9%, 9.2%.

c Ratio 408/488nm and Bright Field images for wild type, *ced-3(-)*, *fasn-1(D/E)*

Grx1-roGFP2 GSSG/GSH Ratio Fold Change; *p=0.0008* (wild type vs *ced-3(-)*), *p=0.0031* (wild type vs *fasn-1(D/E)*)

d Carnitine Synthesis — No stress, ER stress, Osmotic stress, ROS stress; wild type, *ced-3(-)*, *fasn-1(D/E)*. Metabolites: Ascorbic acid, Acetylcarnitine, S-Adenosylhomocysteine, Oxoglutaric acid, Pyridoxal 5'-phosphate, Glycine, Lysine. Log2FC to WT No Stress (<-2 to >2).

e Beta-Alanine Metabolism — No stress, ER stress, Osmotic stress, ROS stress; wild type, *ced-3(-)*, *fasn-1(D/E)*. Metabolites: Ureidopropionic acid, Histidine, Oxoglutaric acid, Pantothenic acid, Uracil, NAD, FAD, NADH, Pyridoxal 5'-phosphate, Flavin mononucleotide. Log2FC to WT No Stress (<-2 to >2).

f Mouse caspase-3; Total Protein Level fold change; Veh vs H_2O_2; *p=0.4586*

g GSSG/GSH Ratio; Stress: No, ER, Osmotic, ROS; *p=0.0087*, *p=0.0022*, *p=0.0649*

Extended Data Fig. 6 | See next page for caption.

Extended Data Fig. 6 | Effect of *ced-3(-)* and *fasn-1(D/E)* mutation on metabolism with diverse stressors. a, Pearson's analysis of metabolites changed in *fasn-1(D/E)* and *ced-3(-)* null mutants compared to wild type animals with no stress treatment. **b**, eigenvalues of PCA analysis for wild type, *ced-3(-)* and *fasn-1(D/E)* mutant with no stress treatment and each of the ER, osmotic and ROS stress. **c**, images and quantification of Grx1-roGFP2 ratio in wild type, *ced-3(-)* and *fasn-1(D/E)* under no stress condition. Excitation of 408 nm was used to estimate GSSG and excitation of 488 nm was used to estimate GSH. Ratio-metric images of the two channels was generated using Fiji (Image J v 1.54 f). Scale bar, 200 μm. WT n = 17, *ced-3(-)* and *fasn-1(D/E)* n = 20. **d-e**, heatmap of detected metabolites in carnitine synthesis (**d**) and beta-alanine metabolism (**e**) pathway. Log$_2$-fold change relative to mean value of wild type no stress. n = 6 biological replicates. **f**, total caspase-3 protein detected in lysate. Average of vehicle treated set to 1, n = 3. Mean ± SD. **g**, GSSG/GSH ratio of wild type animals under diverse stress conditions. n = 6 biological replicates. Mean ± SD. Data from untargeted metabolomics. *p* values were calculated using Mann-Whitney, two-tailed test (**c,g**) or unpaired, two-tailed t-test (**f**).
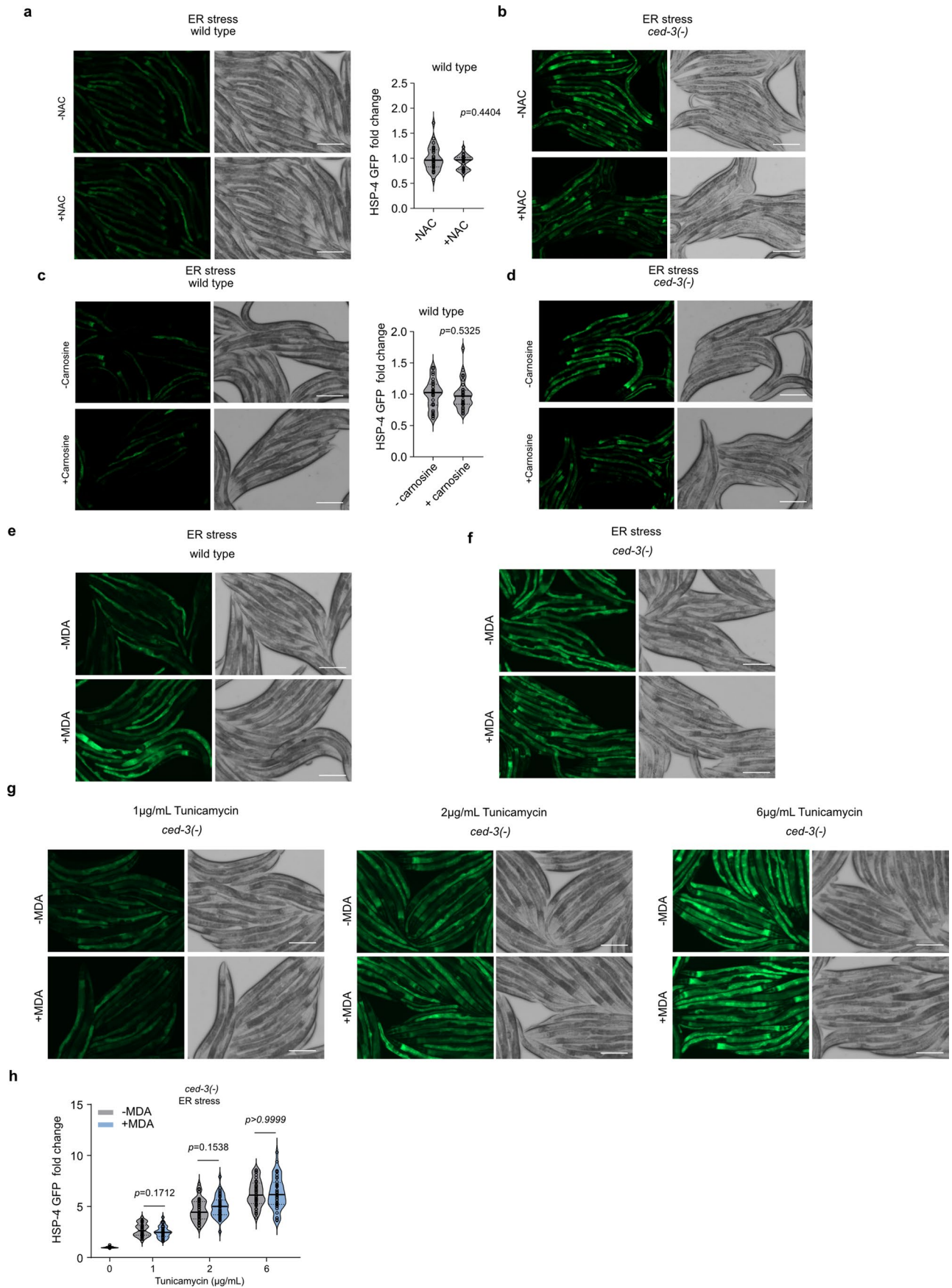
Extended Data Fig. 7 | See next page for caption.

Extended Data Fig. 7 | Extended Data Fig.7 Cellular oxidative state alters caspase-mediated stress responsiveness. a, representative images of HSP-4p::GFP stress reporter induction under ER stress with N-acetylcysteine (NAC) supplementation in wild type animals. Quantification n = 30 animals. **b**, representative images of HSP-4p::GFP stress reporter induction under ER stress with NAC supplementation in *ced-3(-)* animals. Quantification shown in main Fig. 3. **c**, representative images of HSP-4p::GFP stress reporter induction under ER stress with carnosine supplementation in wild type animals. Quantification n = 30 animals. **d**, representative images of HSP-4p::GFP stress reporter induction under ER stress with carnosine supplementation in *ced-3(-)* animals. Quantification shown in main Fig. 3. **e-f**, representative images of HSP-4p::GFP stress reporter induction under ER stress with MDA (malondialdehyde) supplementation in wild type animals (**e**) and *ced-3(-)* animals (**f**). Quantification shown in main Fig. 3. **g-h**, representative images (**g**) and quantification (**h**) of HSP-4p::GFP stress reporter induction under increasing tunicamycin concentration with MDA (malondialdehyde) supplementation in *ced-3(-)* animals. n = 40 animals. *p* values were calculated using Mann-Whitney, two-tailed test (**a,c,h**). Scale bar, 200μm (**a,b,c,d,e,f,g**).
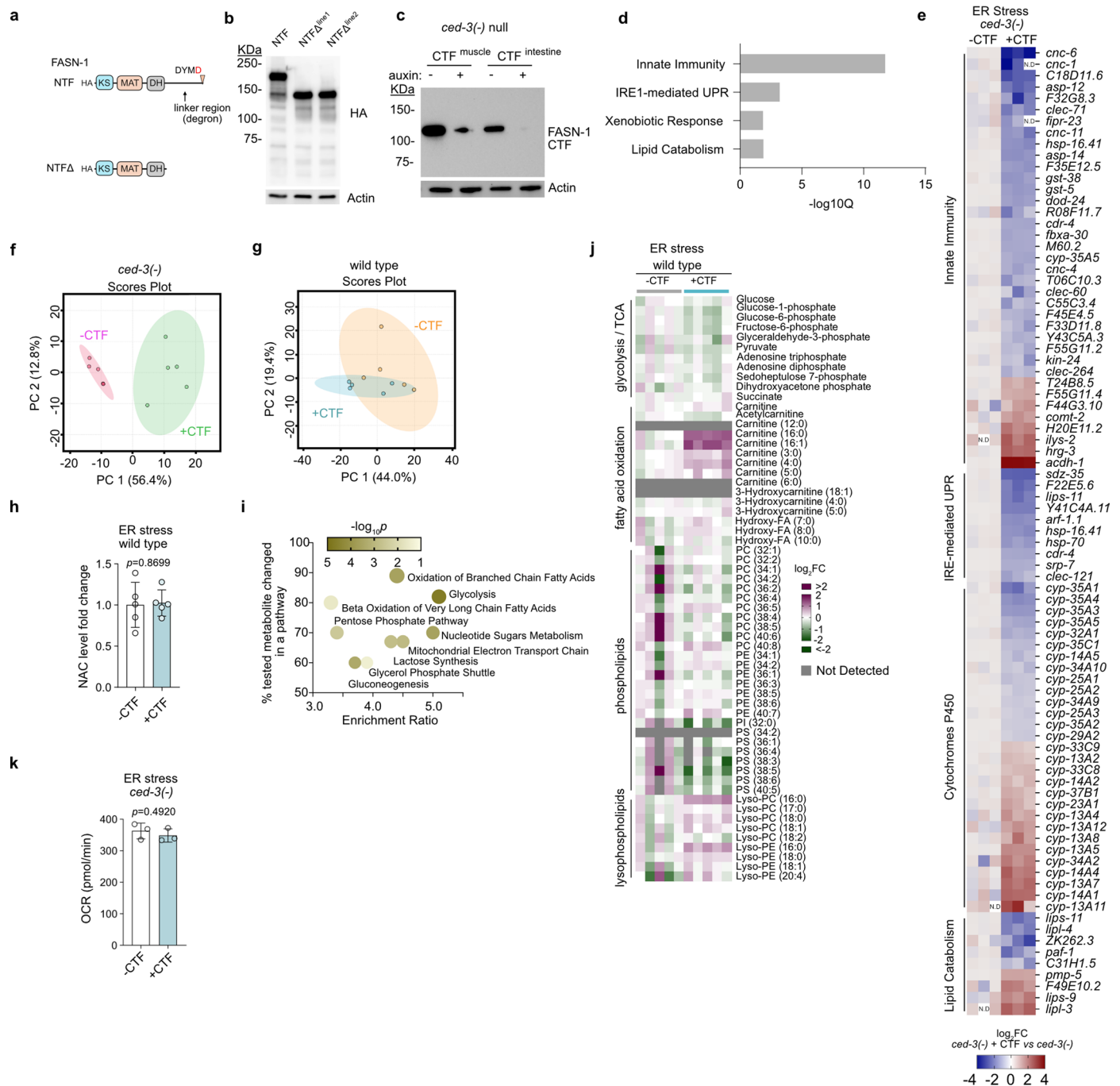
Extended Data Fig. 8 | Impact of FASN-CTF on gene expression and metabolic profiles. a, diagram showing the location of FASN-NTF linker region which is a degron. NTFΔ is FASN-NTF with the linker region removed. **b**, Western blot of FASN-NTF showing the band near 150 kDa corresponds to removal of the linker region (NTFΔ). Western blot was performed once to confirm FASN-NTF linker region is a degron as shown in Fig. 4a. **c**, Western blot of tissue specific CTF expression controlled by auxin. Western blot was performed once to show expression. **d**, FASN-CTF alters gene expression of *ced-3(-)* null mutants pathway enrichments –log10Q value. Enrichment analysis was performed using Enrichment Analysis tool from WormBase (https://wormbase.org/tools/enrichment/tea/tea.cgi). **e**, Heatmap of genes in enriched pathways with FDR < 0.1. n = 3 biological replicates. Log₂ fold change of *ced-3(-)* expressing CTF compared to *ced-3(-)* with no CTF. **f**, PCA analysis for targeted metabolomics of *ced-3(-)* expressing CTF (green) compared to *ced-3(-)* with no CTF (purple). **g**, PCA analysis for targeted metabolomics of wild type animals expressing CTF (green) compared to wild type with no CTF (orange). **h**, N-acetylcysteine (NAC) level in wild type animals with and without CTF expression. n = 5 biological replicates. Mean ± SD. **i**, Enrichment analysis of targeted metabolomics of *ced-3(-)* expressing CTF compared to *ced-3(-)* with no CTF using MetaboAnalyst (https://www.metaboanalyst.ca/) with SMPDB. **j**, heatmap of wild type animals expressing CTF under ER stress showing Log₂FC of the same metabolites shown in Fig. 4j. n = 5 biological replicates. **k**, OCR analysis of *ced-3(-)* mutant expressing CTF compared to *ced-3(-)* with no CTF expression. n = 3 biological replicates. Mean ± SD. *p* values were calculated using unpaired, two-tailed t-test (**h,k**) or one-tailed Fisher's exact test (**i**).
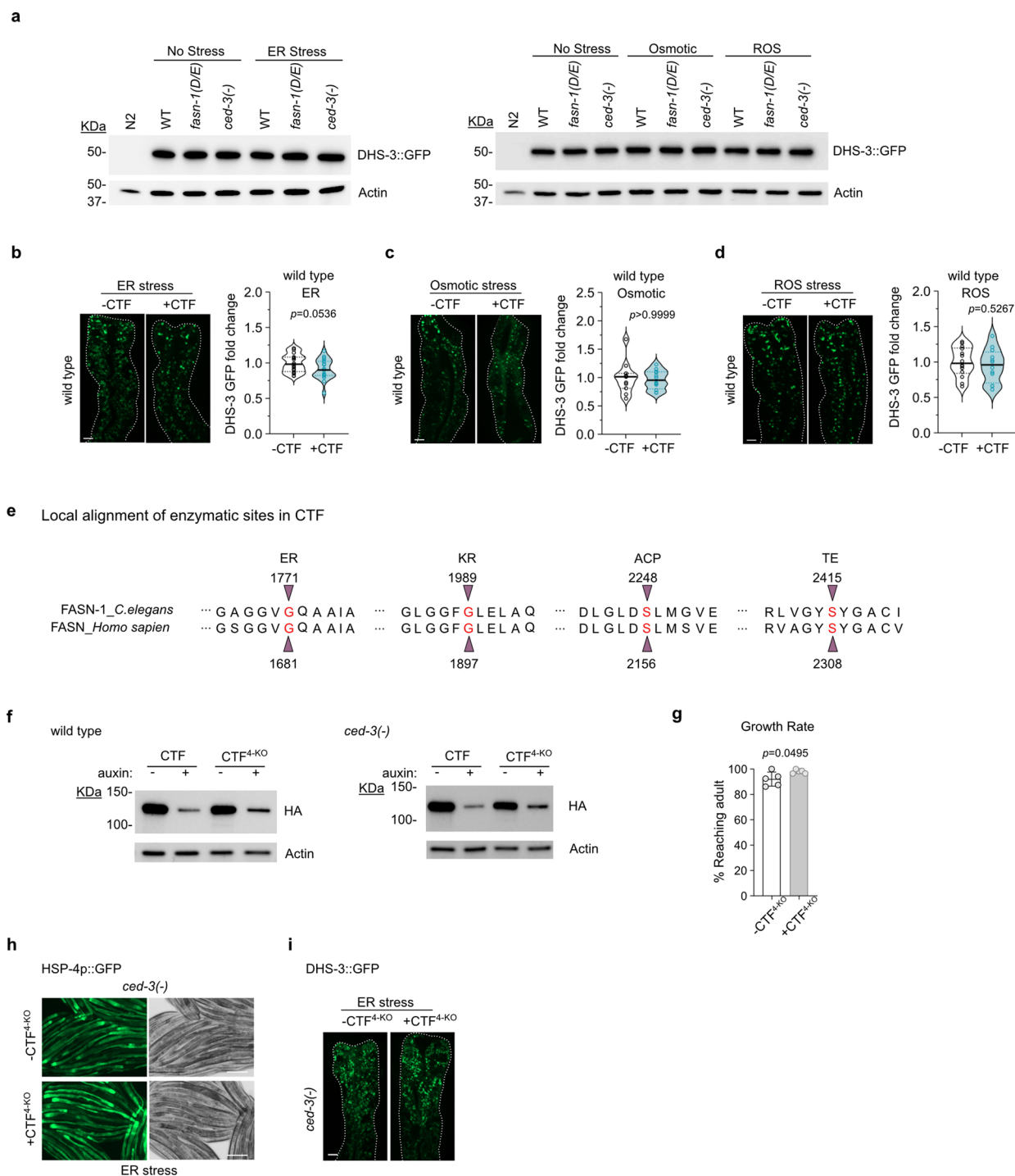
Extended Data Fig. 9 | Impact of FASN-CTF on lipid droplet dynamics and characterization of FASN-CTF⁴⁻ᴷᴼ. a, Western blot analysis showing no effect on DHS-3::GFP protein accumulation by ced-3(-) or fasn-1(D/E) mutants with or without diverse stressors. Western blot was performed once to show no difference in expression. **b-d,** lipid droplets with expression of FASN-CTF in wild type animals under ER stress (**b**), n = 19 animals with CTF and 20 animals without CTF; osmotic stress (**c**), n = 12 animals with CTF and 11 animals without CTF and ROS stress (**d**), n = 12 animals with CTF and 14 animals without CTF. **e,** local sequence alignment of FASN-CTF with four point mutations that inactivate the four enzymatic domains (FASN-CTF⁴⁻ᴷᴼ). **f,** Western blot showing auxin-controlled expression of FASN-CTF and FASN-CTF⁴⁻ᴷᴼ in wild type and

ced-3(-) animals. Western blot was performed once to show no difference in expression. **g,** no delay in growth rate with expression of FASN-CTF⁴⁻ᴷᴼ. Percent of animals reaching young adulthood 62 hours after synchronized egg laying. n = 5 biological replicates. Mean ± SD. **h,** representative image of induction of ER stress marker HSP-4p::GFP with expression of FASN-CTF⁴⁻ᴷᴼ under ER stress in ced-3(-) mutant animals. Quantification shown in main Fig. 6b. **i,** representative image induction of lipid droplet marker DHS-3p::GFP with expression of FASN-CTF⁴⁻ᴷᴼ under ER stress in ced-3(-) mutant animals. Quantification shown in main Fig. 6c. p values were calculated using Mann-Whitney, two-tailed test (**b,c,d**) or unpaired, two-tailed t-test (**g**). Scale bar, 10μm (**b,c,d,i**) and 200μm (**h**).
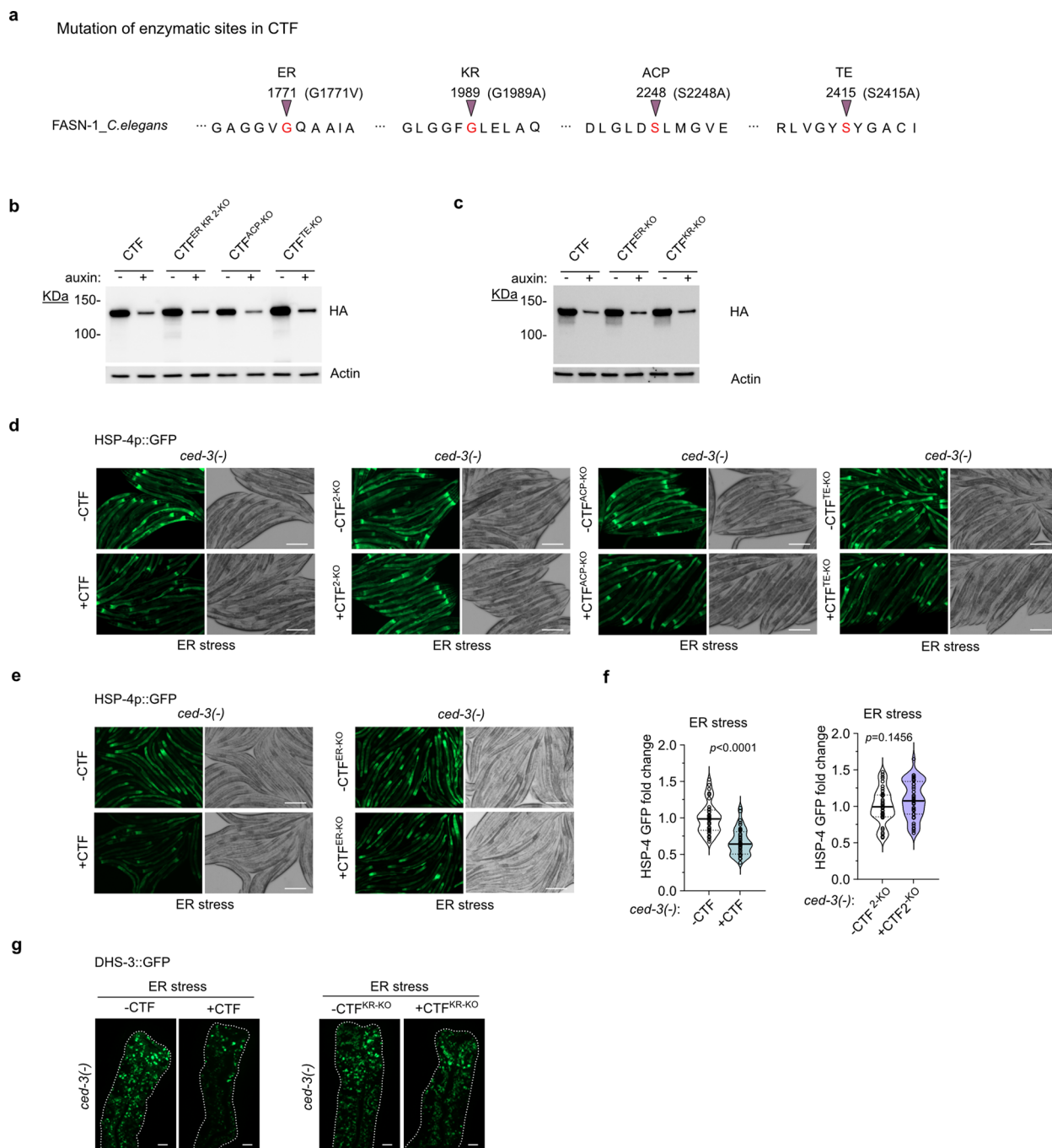
Extended Data Fig. 10 | Characterization of FASN-CTF point mutations in individual enzymatic domain. a, local sequence with 4 point mutations that inactivate the four enzymatic domains. Single point mutations were generated to inactivate one site at a time. **b-c**, Western blots showing auxin-controlled expression of FASN-CTF point mutations including ER-KO (G1771V) KR-KO(G1989A), ACP-KO(S2248A), TE-KO(S2415A) and ER KR-2KO (G1771V, G1989A). Western blots were performed once to show no difference in expression. **d-e**, representative image of induction of ER stress marker HSP-4p::GFP with expression of FASN-CTF point mutations under ER stress in *ced-3(-)* mutant animals. Quantification shown in main Fig. 6g-i. **f**, Quantification of ER stress marker HSP-4p::GFP with expression of FASN-CTF point mutation ER KR-2KO (enoyl reductase and ketoacyl reductase domain mutants) and wild type FASN-CTF control under ER stress. n = 40 animals per condition. *p* values were calculated using Mann-Whitney, two-tailed test. **g**, representative image induction of lipid droplet marker DHS-3p::GFP with expression of FASN-CTF^KR-KO under ER stress in *ced-3(-)* mutant animals. Quantification shown in Fig. 6l. Scale bar, 200μm (**d,e**) and 10μm (**g**).

Corresponding author(s): Benjamin P Weaver

Last updated by author(s): Oct 10, 2023

Reporting Summary

Nature Portfolio wishes to improve the reproducibility of the work that we publish. This form provides structure for consistency and transparency in reporting. For further information on Nature Portfolio policies, see our Editorial Policies and the Editorial Policy Checklist.

Statistics

For all statistical analyses, confirm that the following items are present in the figure legend, table legend, main text, or Methods section.

n/a	Confirmed	
☐	☒	The exact sample size (*n*) for each experimental group/condition, given as a discrete number and unit of measurement
☐	☒	A statement on whether measurements were taken from distinct samples or whether the same sample was measured repeatedly
☐	☒	The statistical test(s) used AND whether they are one- or two-sided *Only common tests should be described solely by name; describe more complex techniques in the Methods section.*
☐	☒	A description of all covariates tested
☒	☐	A description of any assumptions or corrections, such as tests of normality and adjustment for multiple comparisons
☐	☒	A full description of the statistical parameters including central tendency (e.g. means) or other basic estimates (e.g. regression coefficient) AND variation (e.g. standard deviation) or associated estimates of uncertainty (e.g. confidence intervals)
☐	☒	For null hypothesis testing, the test statistic (e.g. F, t, r) with confidence intervals, effect sizes, degrees of freedom and *P* value noted *Give P values as exact values whenever suitable.*
☒	☐	For Bayesian analysis, information on the choice of priors and Markov chain Monte Carlo settings
☐	☒	For hierarchical and complex designs, identification of the appropriate level for tests and full reporting of outcomes
☐	☒	Estimates of effect sizes (e.g. Cohen's *d*, Pearson's *r*), indicating how they were calculated

Our web collection on statistics for biologists contains articles on many of the points above.

Software and code

Policy information about availability of computer code

Data collection	TraceFinder (ThermoScientific) for manual peak integration for metabolomics. Zeiss Zen Imaging software v_2.5 and v_3.4 Pro for image collection. BioRad ChemiDoc MP imaging system for Western. Typhoon FLA 7000 GE for phosphorimaging.
Data analysis	GraphPad Prism 9 for statistics. MetaboAnalyst 5.0 (https://www.metaboanalyst.ca) for metabolomics. WormBase (https://wormbase.org/) for gene enrichment analyses. For mRNA seq, single-end 76 bp read length Fastq files were checked for quality using fastqc (v0.11.2) and fastq_screen (v0.4.4).Reads were quality trimmed using fastq-mcf (ea-utils, v1.1.2-806).Trimmed fastq files were mapped to C elegans genome using STAR (v2.5.3a).Duplicate alignments were removed using picard-tools(v2.10).Read counts were generated using featureCounts (subread) for coding genes from igenomes (Refseq). Normalized read counts generated using edgeR. Fluorescence quantifications were processed using Fiji (1.54f)

For manuscripts utilizing custom algorithms or software that are central to the research but not yet described in published literature, software must be made available to editors and reviewers. We strongly encourage code deposition in a community repository (e.g. GitHub). See the Nature Portfolio guidelines for submitting code & software for further information.

Data

All manuscripts must include a data availability statement. This statement should provide the following information, where applicable:

- Accession codes, unique identifiers, or web links for publicly available datasets
- A description of any restrictions on data availability
- For clinical datasets or third party data, please ensure that the statement adheres to our policy

The mRNA-Seq data generated in this study have been deposited in the GEO database under accession code GSE226048. The remaining data generated in this study are provided in the Source Data file. Source data are provided with this paper.

Research involving human participants, their data, or biological material

Policy information about studies with human participants or human data. See also policy information about sex, gender (identity/presentation), and sexual orientation and race, ethnicity and racism.

Reporting on sex and gender	N/A
Reporting on race, ethnicity, or other socially relevant groupings	N/A
Population characteristics	N/A
Recruitment	N/A
Ethics oversight	N/A

Note that full information on the approval of the study protocol must also be provided in the manuscript.

Field-specific reporting

Please select the one below that is the best fit for your research. If you are not sure, read the appropriate sections before making your selection.

☒ Life sciences   ☐ Behavioural & social sciences   ☐ Ecological, evolutionary & environmental sciences

For a reference copy of the document with all sections, see nature.com/documents/nr-reporting-summary-flat.pdf

Life sciences study design

All studies must disclose on these points even when the disclosure is negative.

Sample size	No statistical methods were used to pre-determine sample sizes but our sample sizes are similar to those reported in previous publications.
Data exclusions	No data were excluded.
Replication	For mRNA seq analyses, biological replicates of 3 samples with tens of thousands of worms in each replicate were used throughout. For metabolomics, biological replicates of 5 to 6 samples with tens of thousands of worms in each replicate. For image analyses, individual measurements of 6 to 40 animals were made for each condition depending on the assay. For Seahorse experiments, 3 biological replicates with with tens of thousands of worms in each replicate. Phenotype assays had 3 to 5 replicates with around 100 animals per genotype for each experiment. Growth assays had 5 replicates with 20 to 100 worms per replicate. All experiments are replicated with measurements of independent biological replicates All replicates data are shown throughout as either dot plots or bar with standard deviation. All attempts at replication were successful. All data variation are shown throughout.
Randomization	For experiments comparing strains with defined genetic background, randomization was not relevant. For experiments comparing different treatments of the same genetic background, all worms used in the various conditions were derived from the same preceding parental plate. If fluorescent markers were used for evaluation, animals were pre-selected under bright light only. When only a portion of animals in the experiment were scored due to throughput limit of an assay (e.g. growth, survival , etc), animals were scored in a pre-determined grid from left to right and top to bottom order with all animals in the grid recorded and reported.
Blinding	Data collection and analysis were not performed blind to the conditions of the experiments.

Behavioural & social sciences study design

All studies must disclose on these points even when the disclosure is negative.

Study description	*Briefly describe the study type including whether data are quantitative, qualitative, or mixed-methods (e.g. qualitative cross-sectional, quantitative experimental, mixed-methods case study).*
Research sample	*State the research sample (e.g. Harvard university undergraduates, villagers in rural India) and provide relevant demographic information (e.g. age, sex) and indicate whether the sample is representative. Provide a rationale for the study sample chosen. For studies involving existing datasets, please describe the dataset and source.*
Sampling strategy	*Describe the sampling procedure (e.g. random, snowball, stratified, convenience). Describe the statistical methods that were used to predetermine sample size OR if no sample-size calculation was performed, describe how sample sizes were chosen and provide a rationale for why these sample sizes are sufficient. For qualitative data, please indicate whether data saturation was considered, and what criteria were used to decide that no further sampling was needed.*
Data collection	*Provide details about the data collection procedure, including the instruments or devices used to record the data (e.g. pen and paper, computer, eye tracker, video or audio equipment) whether anyone was present besides the participant(s) and the researcher, and whether the researcher was blind to experimental condition and/or the study hypothesis during data collection.*
Timing	*Indicate the start and stop dates of data collection. If there is a gap between collection periods, state the dates for each sample cohort.*
Data exclusions	*If no data were excluded from the analyses, state so OR if data were excluded, provide the exact number of exclusions and the rationale behind them, indicating whether exclusion criteria were pre-established.*
Non-participation	*State how many participants dropped out/declined participation and the reason(s) given OR provide response rate OR state that no participants dropped out/declined participation.*
Randomization	*If participants were not allocated into experimental groups, state so OR describe how participants were allocated to groups, and if allocation was not random, describe how covariates were controlled.*

Ecological, evolutionary & environmental sciences study design

All studies must disclose on these points even when the disclosure is negative.

Study description	*Briefly describe the study. For quantitative data include treatment factors and interactions, design structure (e.g. factorial, nested, hierarchical), nature and number of experimental units and replicates.*
Research sample	*Describe the research sample (e.g. a group of tagged Passer domesticus, all Stenocereus thurberi within Organ Pipe Cactus National Monument), and provide a rationale for the sample choice. When relevant, describe the organism taxa, source, sex, age range and any manipulations. State what population the sample is meant to represent when applicable. For studies involving existing datasets, describe the data and its source.*
Sampling strategy	*Note the sampling procedure. Describe the statistical methods that were used to predetermine sample size OR if no sample-size calculation was performed, describe how sample sizes were chosen and provide a rationale for why these sample sizes are sufficient.*
Data collection	*Describe the data collection procedure, including who recorded the data and how.*
Timing and spatial scale	*Indicate the start and stop dates of data collection, noting the frequency and periodicity of sampling and providing a rationale for these choices. If there is a gap between collection periods, state the dates for each sample cohort. Specify the spatial scale from which the data are taken*
Data exclusions	*If no data were excluded from the analyses, state so OR if data were excluded, describe the exclusions and the rationale behind them, indicating whether exclusion criteria were pre-established.*
Reproducibility	*Describe the measures taken to verify the reproducibility of experimental findings. For each experiment, note whether any attempts to repeat the experiment failed OR state that all attempts to repeat the experiment were successful.*
Randomization	*Describe how samples/organisms/participants were allocated into groups. If allocation was not random, describe how covariates were controlled. If this is not relevant to your study, explain why.*
Blinding	*Describe the extent of blinding used during data acquisition and analysis. If blinding was not possible, describe why OR explain why blinding was not relevant to your study.*

Did the study involve field work? ☐ Yes ☒ No

Reporting for specific materials, systems and methods

We require information from authors about some types of materials, experimental systems and methods used in many studies. Here, indicate whether each material, system or method listed is relevant to your study. If you are not sure if a list item applies to your research, read the appropriate section before selecting a response.

Materials & experimental systems

n/a	Involved in the study
☐	☒ Antibodies
☒	☐ Eukaryotic cell lines
☒	☐ Palaeontology and archaeology
☐	☒ Animals and other organisms
☒	☐ Clinical data
☒	☐ Dual use research of concern
☒	☐ Plants

Methods

n/a	Involved in the study
☒	☐ ChIP-seq
☒	☐ Flow cytometry
☒	☐ MRI-based neuroimaging

Antibodies

Antibodies used	HA-Tag (C29F4) Rabbit mAb (Cell Signaling Technology, 3724S), hFAB™ Rhodamine Anti-Actin (Bio-Rad, 12004163), Mouse mAb (Cell Signaling Technology, 2367S)
Validation	HA-Tag (C29F4) Rabbit mAb (Cell Signaling TechnologyCat#3724),Validation provided by supplier_https://www.cellsignal.com/products/primary-antibodies/ha-tag-c29f4-rabbit-mab/3724; Validated in our lab for C elegans species in western blot (Extended Data Fig 3d). hFAB™ Rhodamine Anti-Actin (Bio-RadCat#12004163),Validation provided by supplier_https://www.bio-rad.com/en-us/sku/12004163-hfab-rhodamine-anti-actin-primary-antibody-200-ul?ID=12004163; Mouse mAb (Cell Signaling Technology, 2367S), Validation provided by supplier_https://www.cellsignal.com/products/primary-antibodies/ha-tag-6e2-mouse-mab/2367

Eukaryotic cell lines

Policy information about cell lines and Sex and Gender in Research

Cell line source(s)	*State the source of each cell line used and the sex of all primary cell lines and cells derived from human participants or vertebrate models.*
Authentication	*Describe the authentication procedures for each cell line used OR declare that none of the cell lines used were authenticated.*
Mycoplasma contamination	*Confirm that all cell lines tested negative for mycoplasma contamination OR describe the results of the testing for mycoplasma contamination OR declare that the cell lines were not tested for mycoplasma contamination.*
Commonly misidentified lines (See ICLAC register)	*Name any commonly misidentified cell lines used in the study and provide a rationale for their use.*

Palaeontology and Archaeology

Specimen provenance	*Provide provenance information for specimens and describe permits that were obtained for the work (including the name of the issuing authority, the date of issue, and any identifying information). Permits should encompass collection and, where applicable, export.*
Specimen deposition	*Indicate where the specimens have been deposited to permit free access by other researchers.*
Dating methods	*If new dates are provided, describe how they were obtained (e.g. collection, storage, sample pretreatment and measurement), where they were obtained (i.e. lab name), the calibration program and the protocol for quality assurance OR state that no new dates are provided.*

☐ Tick this box to confirm that the raw and calibrated dates are available in the paper or in Supplementary Information.

Ethics oversight	*Identify the organization(s) that approved or provided guidance on the study protocol, OR state that no ethical approval or guidance was required and explain why not.*

Note that full information on the approval of the study protocol must also be provided in the manuscript.

Animals and other research organisms

Policy information about [studies involving animals](); [ARRIVE guidelines]() recommended for reporting animal research, and [Sex and Gender in Research]()

Laboratory animals	C elegans strains originally derived from N2 Bristol background of 78 different genotypes used were used in this study. Strain names and genotypes provided in Supplementary Table.1. Ages of C elegans from hatching to day 1 young adult as indicated per experiment. Genotypes confirmed by sequence analysis with primers outside of the homologous region. Wild-type males on C57BL/6J mice were used. Age 16 weeks.
Wild animals	No wild animals were used in the study
Reporting on sex	C elegans hermaphrodites were used throughout. For mice, male mice were used.
Field-collected samples	No field-collected samples were used in the study
Ethics oversight	All animal use was approved by the Institutional Animal Care and Use Committee (IACUC) at the University of Texas Southwestern Medical Center Dallas.

Note that full information on the approval of the study protocol must also be provided in the manuscript.

Clinical data

Policy information about [clinical studies]()
All manuscripts should comply with the ICMJE [guidelines for publication of clinical research]() and a completed [CONSORT checklist]() must be included with all submissions.

Clinical trial registration	*Provide the trial registration number from ClinicalTrials.gov or an equivalent agency.*
Study protocol	*Note where the full trial protocol can be accessed OR if not available, explain why.*
Data collection	*Describe the settings and locales of data collection, noting the time periods of recruitment and data collection.*
Outcomes	*Describe how you pre-defined primary and secondary outcome measures and how you assessed these measures.*

Dual use research of concern

Policy information about [dual use research of concern]()

Hazards

Could the accidental, deliberate or reckless misuse of agents or technologies generated in the work, or the application of information presented in the manuscript, pose a threat to:

No	Yes	
☒	☐	Public health
☒	☐	National security
☒	☐	Crops and/or livestock
☒	☐	Ecosystems
☒	☐	Any other significant area

Experiments of concern

Does the work involve any of these experiments of concern:

No	Yes	
☒	☐	Demonstrate how to render a vaccine ineffective
☒	☐	Confer resistance to therapeutically useful antibiotics or antiviral agents
☒	☐	Enhance the virulence of a pathogen or render a nonpathogen virulent
☒	☐	Increase transmissibility of a pathogen
☒	☐	Alter the host range of a pathogen
☒	☐	Enable evasion of diagnostic/detection modalities
☒	☐	Enable the weaponization of a biological agent or toxin
☒	☐	Any other potentially harmful combination of experiments and agents

Plants

Seed stocks	*Report on the source of all seed stocks or other plant material used. If applicable, state the seed stock centre and catalogue number. If plant specimens were collected from the field, describe the collection location, date and sampling procedures.*
Novel plant genotypes	*Describe the methods by which all novel plant genotypes were produced. This includes those generated by transgenic approaches, gene editing, chemical/radiation-based mutagenesis and hybridization. For transgenic lines, describe the transformation method, the number of independent lines analyzed and the generation upon which experiments were performed. For gene-edited lines, describe the editor used, the endogenous sequence targeted for editing, the targeting guide RNA sequence (if applicable) and how the editor was applied.*
Authentication	*Describe any authentication procedures for each seed stock used or novel genotype generated. Describe any experiments used to assess the effect of a mutation and, where applicable, how potential secondary effects (e.g. second site T-DNA insertions, mosiacism, off-target gene editing) were examined.*

ChIP-seq

Data deposition

☐ Confirm that both raw and final processed data have been deposited in a public database such as GEO.

☐ Confirm that you have deposited or provided access to graph files (e.g. BED files) for the called peaks.

Data access links *May remain private before publication.*	*For "Initial submission" or "Revised version" documents, provide reviewer access links. For your "Final submission" document, provide a link to the deposited data.*
Files in database submission	*Provide a list of all files available in the database submission.*
Genome browser session (e.g. UCSC)	*Provide a link to an anonymized genome browser session for "Initial submission" and "Revised version" documents only, to enable peer review. Write "no longer applicable" for "Final submission" documents.*

Methodology

Replicates	*Describe the experimental replicates, specifying number, type and replicate agreement.*
Sequencing depth	*Describe the sequencing depth for each experiment, providing the total number of reads, uniquely mapped reads, length of reads and whether they were paired- or single-end.*
Antibodies	*Describe the antibodies used for the ChIP-seq experiments; as applicable, provide supplier name, catalog number, clone name, and lot number.*
Peak calling parameters	*Specify the command line program and parameters used for read mapping and peak calling, including the ChIP, control and index files used.*
Data quality	*Describe the methods used to ensure data quality in full detail, including how many peaks are at FDR 5% and above 5-fold enrichment.*
Software	*Describe the software used to collect and analyze the ChIP-seq data. For custom code that has been deposited into a community repository, provide accession details.*

Flow Cytometry

Plots

Confirm that:

☐ The axis labels state the marker and fluorochrome used (e.g. CD4-FITC).

☐ The axis scales are clearly visible. Include numbers along axes only for bottom left plot of group (a 'group' is an analysis of identical markers).

☐ All plots are contour plots with outliers or pseudocolor plots.

☐ A numerical value for number of cells or percentage (with statistics) is provided.

Methodology

Sample preparation

> *Describe the sample preparation, detailing the biological source of the cells and any tissue processing steps used.*

Instrument

> *Identify the instrument used for data collection, specifying make and model number.*

Software

> *Describe the software used to collect and analyze the flow cytometry data. For custom code that has been deposited into a community repository, provide accession details.*

Cell population abundance

> *Describe the abundance of the relevant cell populations within post-sort fractions, providing details on the purity of the samples and how it was determined.*

Gating strategy

> *Describe the gating strategy used for all relevant experiments, specifying the preliminary FSC/SSC gates of the starting cell population, indicating where boundaries between "positive" and "negative" staining cell populations are defined.*

☐ Tick this box to confirm that a figure exemplifying the gating strategy is provided in the Supplementary Information.

Magnetic resonance imaging

Experimental design

Design type

> *Indicate task or resting state; event-related or block design.*

Design specifications

> *Specify the number of blocks, trials or experimental units per session and/or subject, and specify the length of each trial or block (if trials are blocked) and interval between trials.*

Behavioral performance measures

> *State number and/or type of variables recorded (e.g. correct button press, response time) and what statistics were used to establish that the subjects were performing the task as expected (e.g. mean, range, and/or standard deviation across subjects).*

Acquisition

Imaging type(s)

> *Specify: functional, structural, diffusion, perfusion.*

Field strength

> *Specify in Tesla*

Sequence & imaging parameters

> *Specify the pulse sequence type (gradient echo, spin echo, etc.), imaging type (EPI, spiral, etc.), field of view, matrix size, slice thickness, orientation and TE/TR/flip angle.*

Area of acquisition

> *State whether a whole brain scan was used OR define the area of acquisition, describing how the region was determined.*

Diffusion MRI   ☐ Used   ☐ Not used

Preprocessing

Preprocessing software

> *Provide detail on software version and revision number and on specific parameters (model/functions, brain extraction, segmentation, smoothing kernel size, etc.).*

Normalization

> *If data were normalized/standardized, describe the approach(es): specify linear or non-linear and define image types used for transformation OR indicate that data were not normalized and explain rationale for lack of normalization.*

Normalization template

> *Describe the template used for normalization/transformation, specifying subject space or group standardized space (e.g. original Talairach, MNI305, ICBM152) OR indicate that the data were not normalized.*

Noise and artifact removal

> *Describe your procedure(s) for artifact and structured noise removal, specifying motion parameters, tissue signals and physiological signals (heart rate, respiration).*

Volume censoring | *Define your software and/or method and criteria for volume censoring, and state the extent of such censoring.*

Statistical modeling & inference

Model type and settings | *Specify type (mass univariate, multivariate, RSA, predictive, etc.) and describe essential details of the model at the first and second levels (e.g. fixed, random or mixed effects; drift or auto-correlation).*

Effect(s) tested | *Define precise effect in terms of the task or stimulus conditions instead of psychological concepts and indicate whether ANOVA or factorial designs were used.*

Specify type of analysis: ☐ Whole brain ☐ ROI-based ☐ Both

Statistic type for inference | *Specify voxel-wise or cluster-wise and report all relevant parameters for cluster-wise methods.*

(See Eklund et al. 2016)

Correction | *Describe the type of correction and how it is obtained for multiple comparisons (e.g. FWE, FDR, permutation or Monte Carlo).*

Models & analysis

n/a	Involved in the study
☐	☐ Functional and/or effective connectivity
☐	☐ Graph analysis
☐	☐ Multivariate modeling or predictive analysis

Functional and/or effective connectivity | *Report the measures of dependence used and the model details (e.g. Pearson correlation, partial correlation, mutual information).*

Graph analysis | *Report the dependent variable and connectivity measure, specifying weighted graph or binarized graph, subject- or group-level, and the global and/or node summaries used (e.g. clustering coefficient, efficiency, etc.).*

Multivariate modeling and predictive analysis | *Specify independent variables, features extraction and dimension reduction, model, training and evaluation metrics.*